

# Rotationally invariant dynamical lattice regulators for Euclidean quantum field theories

Tsogtgerel Gantumur

McGill University, Montréal, QC, Canada

National University of Mongolia, Ulaanbaatar, Mongolia

Mongolian Academy of Sciences, Institute of Mathematics and Digital Technology

`gantumur.tsogtgerel@mcgill.ca`

January 11, 2026

## Abstract

We introduce a dynamical lattice regulator for Euclidean quantum field theories on a fixed hypercubic graph  $\Lambda \simeq \mathbb{Z}^d$ , in which the embedding  $x : \Lambda \rightarrow \mathbb{R}^d$  is promoted to a dynamical field and integrated over subject to shape regularity constraints. The total action is local on  $\Lambda$ , gauge invariant, and depends on  $x$  only through Euclidean invariants built from edge vectors (local metrics, volumes, *etc.*), hence the partition function is exactly covariant under the global special Euclidean group  $SE(d)$  at any lattice spacing. The intended symmetry restoring mechanism is not rigid global zero modes but short-range *local twisting* of the embedding that mixes local orientations. Our universality discussion is conditioned on a short-range geometry hypothesis (SR): after quotienting the global  $SE(d)$  modes, connected correlators of local geometric observables have correlation length  $O(1)$  in lattice units.

We prove Osterwalder–Schrader reflection positivity for the coupled system with embedding  $x$  and generic gauge and matter fields  $(U, \Phi)$  in finite volume by treating  $x$  as an additional multiplet of scalar fields on  $\Lambda$ . Assuming (SR), integrating out  $x$  at fixed cutoff yields a local Symanzik effective action in which geometry fluctuations generate only  $SO(d)$ -invariant irrelevant operators and finite renormalizations. For example, in  $d = 4$  we recover the standard one-loop  $\beta$ -function in a scalar  $\phi^4$  test theory. Finally, we describe a practical local Monte Carlo update and report  $d = 2$  proof-of-concept simulations showing a well behaved geometry sector and a substantial reduction of axis-vs-diagonal cutoff artefacts relative to a fixed lattice at matched bare parameters.

## Contents

<b>1</b>	<b>Introduction</b>	<b>2</b>
1.1	Motivation . . . . .	2
1.2	Overview of the construction . . . . .	4
1.3	Main results and scope of this paper . . . . .	5
1.4	Comparison to existing approaches . . . . .	6
<b>2</b>	<b>Geometry of the dynamical lattice regulator</b>	<b>8</b>
2.1	Abstract lattice, fields, and embedding . . . . .	8
2.2	Local Euclidean geometry and admissible embeddings . . . . .	9

2.3	Geometry measure and dynamics . . . . .	12
2.4	Torus version and periodic implementation . . . . .	15
<b>3</b>	<b>Field actions and symmetries on a dynamical lattice</b>	<b>15</b>
3.1	Configuration space and full action . . . . .	15
3.2	Euclidean invariance, orientation, and local isotropy . . . . .	19
3.3	Gauge invariance and lattice symmetries . . . . .	23
3.4	Viewpoint as an extended lattice field theory . . . . .	24
<b>4</b>	<b>Reflection positivity and continuum universality</b>	<b>25</b>
4.1	Reflection positivity for the bosonic sector . . . . .	25
4.2	Fermions and reflection positivity . . . . .	29
4.3	Symanzik effective theory and universality . . . . .	32
4.4	Example: one-loop $\beta$ -function in scalar $\phi^4$ theory . . . . .	37
<b>5</b>	<b>Numerical experiments</b>	<b>39</b>
5.1	Simulation protocol . . . . .	39
5.2	Measured observables . . . . .	41
5.3	Geometry sector diagnostics . . . . .	42
5.4	Thermalisation and stability . . . . .	43
5.5	Rotational artefacts: short and intermediate scales . . . . .	43
5.6	Universality and critical scaling . . . . .	43
<b>6</b>	<b>Conclusions and outlook</b>	<b>46</b>
6.1	Future directions . . . . .	46

# 1 Introduction

## 1.1 Motivation

A central difficulty in nonperturbative quantum field theory (QFT) is the tension between the need for an ultraviolet cutoff and the desire to preserve the continuous symmetries of the underlying continuum theory. Wilson’s lattice regularization replaces space–time by a hypercubic graph with lattice spacing  $a$ , and computes expectation values via a Euclidean path integral [1, 2, 3]. This construction is local, gauge invariant, and reflection positive, and it underpins the modern nonperturbative understanding of Yang–Mills theory and quantum chromodynamics. However, it breaks the Euclidean group  $E(d) = O(d) \times \mathbb{R}^d$  down to the discrete hypercubic subgroup. Full Euclidean symmetry is recovered only in the continuum limit, and at finite lattice spacing the reduced symmetry manifests itself as direction–dependent lattice artefacts in correlation functions and derived observables. By “rotational artefacts” we mean precisely this direction dependence at fixed physical separation (e.g. axis versus diagonal separations on the underlying hypercubic stencil), as well as the induced mixing patterns of operators that would be forbidden by continuum  $O(d)$  symmetry but are allowed by the hypercubic subgroup at finite lattice spacing.

Several approaches have been developed to mitigate these symmetry violations. Random lattice methods, dynamical triangulations, and Regge calculus all average over ensembles of discrete geometries [4, 10, 8]. While these ideas show that fluctuating geometry can reduce anisotropy, they typically modify the combinatorial structure of the discretization or sacrifice reflection positivity,

and the randomness is often imposed by an external sampling algorithm or by a gravitational action rather than arising intrinsically from the QFT regulator itself.

The aim of this paper is to develop and analyse a *dynamical lattice regulator* (DLR) for Euclidean QFT that combines the robust structural features of standard lattice gauge theory (locality, exact gauge invariance, Osterwalder–Schrader reflection positivity, and a fixed combinatorial graph) with an exactly (proper) Euclidean–symmetric treatment of geometry already at finite lattice spacing. Concretely, we fix once and for all an abstract hypercubic lattice

$$\Lambda = \mathbb{Z}^d, \tag{1.1}$$

or its finite periodic version for numerical work, which carries the usual gauge and matter fields. We then promote the *embedding* of lattice sites into  $\mathbb{R}^d$  to a dynamical field

$$x : \Lambda \rightarrow \mathbb{R}^d, \quad n \mapsto x(n), \tag{1.2}$$

and integrate  $x$  over in the path integral, subject to local shape–regularity constraints and a local geometry action  $S_x[x]$ . The geometric sector is constructed from Euclidean invariants (distances and inner products), so it is invariant under global translations and proper rotations,

$$\text{SE}(d) = \text{SO}(d) \times \mathbb{R}^d, \tag{1.3}$$

and it is compatible with the specific reflection involution used in the OS positivity proof. However, the mere fact that the partition function is globally  $\text{SE}(d)$ –covariant is, by itself, too weak to address the usual lattice concern: the same formal covariance would also hold if the geometry measure were concentrated near globally rotated/translated copies of a single rigid embedding. What matters for suppressing hypercubic cutoff artefacts is *how* the global symmetry is realised in typical configurations at fixed cutoff.

The operating regime we target is a *short-range geometry* regime (SR). After fixing or quotienting the global  $\text{SE}(d)$  zero modes, typical configurations must exhibit short-range local orientation mixing of the induced frames from cell to cell. In such a regime, global  $\text{SE}(d)$  covariance cannot be realised “rigidly”; it must be implemented through *local twisting*, and it is the one probed in the numerics: neighbours in  $\Lambda$  remain neighbours, but their relative physical orientation varies with short correlation length while their physical separation fluctuates within the admissible range.

From this perspective, random lattices and dynamical triangulations may be viewed as *stochastic topology* models, in which either the connectivity (via Voronoi/Delaunay constructions) or the triangulation itself fluctuates, often driven by an external random point process. In our framework, by contrast, the topology of the lattice is rigid and hypercubic, and it is the embedding  $x$  that fluctuates. The geometric randomness is *internal* to the quantum theory:  $x$  is a genuine dynamical variable governed by a local action inside the same path integral as the gauge and matter fields, not an external pre-processing step.

Our goal in this first work is to show that one can construct a conservative, computationally accessible regulator that

- preserves locality, exact gauge invariance, and reflection positivity;
- is globally  $\text{SE}(d)$ –covariant at finite lattice spacing, and in the twisting regime reduces direction-dependent (axis-vs-diagonal) rotational artefacts relative to a fixed lattice at matched bare parameters;

- is expected to lie in the same universality class as standard hypercubic lattice regulators: perturbatively we verify this at one loop, and in  $d = 2$  we find matching critical scaling between baseline and dynamical ensembles; more generally we formulate a universality statement as Conjecture 4.9 under the short-range geometry hypothesis (SR).

From the lattice QCD viewpoint, the dynamical–lattice regulator may be viewed as an *annealed geometric averaging in coordinate space*, complementary to field–space smoothing techniques such as link smearing and the Wilson flow. In gauge theories we expect such averaging to reduce direction dependent cutoff effects that can “pin” extended or topological structures to the lattice axes, potentially mitigating forms of *topological freezing* at fixed cutoff. At the same time, because the underlying graph topology remains hypercubic, issues such as the fermion doubling are not expected to be resolved by the regulator; the intended benefit for fermions is instead a reduction of anisotropic artefacts (e.g. taste splitting) through orientation mixing. A systematic study of these gauge theory implications is left to future work.

## 1.2 Overview of the construction

We work with an abstract, fixed hypercubic lattice  $\Lambda$ , which would typically be a discrete torus in numerical applications. The usual gauge and matter fields live on  $\Lambda$  exactly as in Wilson’s formulation: link variables  $U_\mu(n) \in G$  on oriented nearest neighbour links, and matter fields  $\Phi(n)$  in some representation of  $G$  on the sites. Here  $n \in \Lambda$  denotes the sites, and  $\mu \in \{1, \dots, d\}$  the spacial directions. The new ingredient is a *geometry field*

$$x : \Lambda \rightarrow \mathbb{R}^d, \tag{1.4}$$

which specifies the physical position  $x(n) \in \mathbb{R}^d$  of each lattice site. From  $x$  we construct local edge vectors, metrics and cell volumes, and we restrict  $x$  to an admissible subset  $\mathcal{X}_{\text{adm}}$  of  $(\mathbb{R}^d)^\Lambda$  by imposing standard shape regularity conditions. The admissible set is chosen so that all local geometries are uniformly comparable to a regular hypercubic mesh with some scale  $a > 0$ .

The full configuration space is thus

$$\mathcal{C} = \mathcal{X}_{\text{adm}} \times G^{\text{links}} \times \mathcal{F}_{\text{matter}}, \tag{1.5}$$

equipped with a product measure  $Dx DU D\Phi$ . A configuration  $(x, U, \Phi) \in \mathcal{C}$  is weighted by a local action

$$S[x, U, \Phi] = S_x[x] + S_{\text{fields}}[x, U, \Phi], \tag{1.6}$$

where  $S_x[x]$  is a geometry action and  $S_{\text{fields}}$  is the usual gauge–matter action written in terms of the local metric and volume induced by  $x$ . Both pieces are built from Euclidean invariants of the embedding data and from gauge invariant combinations of the fields. The resulting theory on  $\mathbb{R}^d$  is globally covariant under translations and proper rotations, i.e., under the special Euclidean group  $\text{SE}(d) = \text{SO}(d) \times \mathbb{R}^d$ . It is also compatible with the discrete reflection involution used in the Osterwalder–Schrader positivity argument, cf. [16, 17]. This statement concerns the unfixed formulation; in practice one may fix the global translation/rotation zero modes without affecting covariant expectations or the local twisting diagnostics.

Standard Wilson lattice gauge theory is recovered as a stiff–geometry limit of the dynamical lattice regulator in which  $S_x[x] = +\infty$  unless  $x = x_{\text{reg}}$ , where  $x_{\text{reg}}(n) = an$  is a regular embedding. This limit is not Euclidean–invariant: freezing the embedding selects a preferred orientation and breaks the continuous Euclidean symmetry explicitly down to the hypercubic symmetry group.

Merely averaging over rigid global rotations of this frozen embedding does not change the local stencil anisotropy; improving isotropy requires fluctuations that mix orientations locally. The novelty is that the geometry remains annealed in a way that preserves locality and the transfer-matrix/OS-positivity framework on the fixed hypercubic graph. This enables local orientation mixing that can suppress hypercubic anisotropies; the stiff (Wilson) limit is recovered by sending the geometry stiffness to infinity.

For conceptual questions (Euclidean covariance, reflection positivity, continuum limit) it is most convenient to formulate the theory on  $\mathbb{R}^d$ , with  $\Lambda$  thought of as an infinite hypercubic lattice and  $x(n) \in \mathbb{R}^d$ . For finite volume simulations we instead interpret  $\Lambda$  as a discrete torus and take  $x(n) \in \mathbb{T}^d$ , using shortest distance representatives to define edge vectors; this torus version is described in §2.4. In both cases the underlying combinatorial graph is kept fixed, while the embedding  $x$  fluctuates subject to admissibility constraints.

Finally, it may help to view the dynamical geometry in purely lattice-theoretic terms. The new variables can be counted as *one additional real scalar per oriented link* (equivalently,  $d$  real numbers per site), while the underlying hypercubic graph, nearest-neighbour stencil, and all gauge/matter variables are exactly those of standard lattice gauge theory. In this repackaging the geometry sector merely promotes certain local couplings to depend on these extra link scalars through  $E(d)$ -invariant combinations (such as distances and inner products), so the regulator enlarges the field content only mildly and in a form that is directly compatible with existing lattice implementations.

### 1.3 Main results and scope of this paper

We summarize the main theoretical and practical conclusions obtained in this paper for dynamical lattice regulators (DLR).

- **Global Euclidean covariance and reflection positivity.** At fixed lattice spacing the coupled theory is exactly  $SE(d)$ -covariant, and we prove Osterwalder–Schrader reflection positivity for a broad class of gauge and matter actions. We distinguish this formal global covariance from the physically relevant notion of reduced direction-dependent cutoff artefacts, which we probe numerically and relate to short-range local twisting.
- **Locality, admissibility and the geometry sector.** We define an admissible set  $\mathcal{X}_{\text{adm}}$  of embeddings by local bounds on edge lengths, angles and orientation, in such a way that the local metrics and volumes are uniformly comparable to those of a regular hypercubic lattice. We discuss the global structure of  $\mathcal{X}_{\text{adm}}$ , the choice of principal component, and simple local Monte Carlo moves for updating  $x$  that preserve admissibility while remaining ergodic within this component.
- **Perturbative universality.** As a first perturbative check we analyze scalar  $\phi^4$  theory on a dynamical lattice. In the Symanzik framework [16, 17], and assuming the short-range geometry hypothesis (SR), integrating out the embedding fluctuations yields a local  $SE(d)$ -invariant effective action: the relevant and marginal operators are therefore the same as in the continuum, while cutoff effects appear only through higher-dimensional  $SO(d)$ -scalar operators. Expanding around a regular embedding  $x(n) = an + \eta(n)$  and treating  $\eta$  as auxiliary fields, we argue that, conditional on (SR), the induced interactions are local and RG-irrelevant. Moreover, at one loop the running of the quartic coupling agrees with that of the standard hypercubic discretization, in line with Conjecture 4.9.

- **Monte Carlo implementation and numerical tests.** We describe a first proof of concept Monte Carlo implementation in  $d = 2$  for a scalar theory on a periodic lattice, using local Metropolis updates for both fields and geometry. Basic observables (masses, susceptibilities) agree with those from a static lattice at the same bare parameters within statistical errors, and simple diagnostics of the geometry sector (edge length, angle and volume distributions) show no pathological concentration on highly distorted meshes. These tests support the claim that the regulator is numerically viable and lies in the expected universality class.

The rest of the paper is organised as follows. In Section 2 we develop the geometry sector: admissible embeddings, local shape-regularity, and Monte Carlo moves. Section 3 introduces the field actions, demonstrates exact  $SE(d)$  invariance, and presents explicit scalar, gauge, and fermion examples. Section 4 establishes reflection positivity and discusses the Symanzik effective theory and continuum universality. Section 5 describes our initial numerical experiments, and Section 6 summarises our findings and outlines possible extensions.

## 1.4 Comparison to existing approaches

The idea of fluctuating geometry in a lattice regularization has a long history. It is therefore important to delineate precisely how the present construction differs from earlier proposals.

**Random and pseudorandom lattices.** In the random lattice (RL) approach, one typically samples a random set of points in a domain  $\Omega \subset \mathbb{R}^d$ , often from a Poisson process, constructs a Voronoi tessellation and its dual Delaunay triangulation, and discretizes the field theory on the resulting random cell complex, cf. [4, 5]. As the points move, the connectivity of the lattice changes discontinuously when Voronoi cells flip; the adjacency matrix is a discontinuous function of the site positions. In this setting the geometry is random, but its law is largely specified by an external stochastic prescription for the points, and reflection positivity is hard to control.

The “pseudorandom lattice” construction of Colangelo *et al.* [6, 7] also aims at improving rotational invariance, but does so while preserving the hypercubic graph: one draws exactly one site inside each elementary hypercubic cell of a reference lattice and connects sites belonging to nearest-neighbour cells. Thus the combinatorial structure and sparsity pattern are the same as on a standard hypercubic lattice, while the geometric embedding (link lengths and angles) is quenched random data chosen once from a tuned probability distribution. This improves the *statistical* isotropy of simple geometric observables, but does not enforce shape regularity or exact  $SE(d)$  symmetry at finite lattice spacing, and the random geometry does not enter as a dynamical field in the same path integral as the gauge and matter sectors.

By contrast, in DLR the abstract hypercubic topology is fixed once and for all. The adjacency relation on  $\Lambda$  does not depend on the embedding  $x$ , and moving the sites never creates or destroys links. What fluctuates is only the embedding

$$x : \Lambda \rightarrow \mathbb{R}^d, \tag{1.7}$$

which is treated as a genuine dynamical field with a local action  $S_x[x]$  in the *same* path integral as the gauge and matter fields. Geometric fluctuations are therefore “annealed” (dynamical) rather than quenched (frozen): the randomness of the geometry is intrinsic to the quantum Lagrangian. Note that we use “annealed” here to refer to the spacetime lattice itself, distinct from the “quenched approximation” regarding fermion loops.

**Regge calculus and dynamical triangulations.** Regge calculus keeps a fixed simplicial connectivity and promotes the edge lengths to dynamical variables, with an action that discretizes the Einstein–Hilbert functional. In dynamical triangulations (DT) and causal dynamical triangulations, one takes a complementary viewpoint: the edge lengths are kept fixed (typically to a few discrete values) and one instead sums over triangulations themselves, so that the gluing pattern of simplices becomes the dynamical variable, again weighted by an Einstein–Hilbert–type action plus matter contributions. In both cases the geometric degrees of freedom are fundamental and the primary goal is to describe quantum gravity [8, 9, 10, 11].

Structurally, DLR is closest to Regge calculus in that it uses a fixed abstract complex together with fluctuating geometric data. There are, however, two important differences. First, the basic variables here are the embedding coordinates  $x(n)$ , from which edge lengths and local metrics are derived; the geometry sector is introduced as an auxiliary regulator field whose role is to restore  $SE(d)$  symmetry and potentially reduce lattice artefacts, not to encode an independent gravitational degree of freedom. Second, the construction is deliberately tied to a hypercubic abstract lattice so as to maintain the locality structure and transfer matrix decomposition of standard lattice gauge theory, which is crucial for the reflection positivity argument and for reusing existing simulation technology. One may view dynamical lattice as a Regge–like dynamics for a fixed hypercubic mesh, with an action tuned for regularization rather than for quantum gravity.

Feature	RL	DT	Regge	DLR
Topology	Stochastic	Stochastic	Simplicial	Hypercubic
Geometry	Random	N/A	Dynamic	Dynamic
Mesh dynamics	External	Gravity	Gravity	Auxiliary
Laplacian	Unstructured	Unstructured	Unstructured	Structured
OS positivity	Generally lost	Generally lost	Lost	Provable

Table 1: Comparison between the random lattice approaches, dynamical triangulations, Regge calculus, and the dynamical lattice regulators.

**Smearing and gradient flow.** Modern lattice gauge theory extensively uses “smearing” techniques that replace the link variables by local averages, as in APE, Stout, or HYP smearing, cf. [12, 13, 14], and the gradient flow that defines a diffusion in field space [15]. These methods replace the oscillating gauge links with locally averaged variables in the definition of operators or the action. While this shares our goal of mitigating UV noise, the mechanism is fundamentally different: smearing smooths the *fields* over a fixed, rigid geometry, whereas DLR smooths the *geometry* itself. By annealing the metric, our approach potentially allows the lattice to accommodate topological objects that might otherwise be frozen by the rigidity of a static grid, a feature that algorithmic smoothing of fields cannot replicate. Equivalently, DLR can be viewed as an *annealed geometric averaging* (or “geometric smearing”): instead of diffusing/smoothing the dynamical fields on a fixed hypercubic background, we diffuse the *coordinate/metric degrees of freedom* seen by the fields by integrating over embeddings. A key difference is that the  $SE(d)$  symmetry is exact at the level of the regulator and partition function (modulo the global zero modes). Smearing/flow improve operators or effective descriptions at finite flow time but do not enlarge the underlying symmetry group of the static lattice regulator beyond the hypercubic subgroup. In this sense DLR realises *intrinsic stochastic rotational averaging* inside the path integral, rather than an external

rotation/projection applied to measured data.

**Improved actions.** Standard lattice regulators rely on the Symanzik improvement program to systematically remove discretization errors by adding higher-dimension irrelevant operators to the action [16, 17]. On a static hypercubic lattice, the breaking of the Euclidean group  $SE(d)$  down to the hypercubic subgroup  $H(d)$  causes single continuum operators to split into multiple lattice operators, e.g., the Laplacian square  $(\partial^2)^2$  splits into rotationally invariant and non-invariant parts. Restoring rotational symmetry to high order therefore requires tuning the coefficients of multiple non-invariant counterterms. In contrast, because DLR preserves exact  $SE(d)$  invariance at finite cutoff, the effective action is constrained to contain only global scalars. This potentially simplifies the improvement program: although the field content is enlarged by the geometry variables, the basis of dangerous irrelevant operators is much smaller. Non-scalar counterterms are forbidden by exact symmetry, meaning one need only tune the coefficients of  $E(d)$ -invariant operators to achieve higher-order accuracy.

**Moving mesh methods.** From the perspective of numerical analysis, the construction is reminiscent of Arbitrary Lagrangian–Eulerian (ALE) and other moving mesh formulations, in which one works with a fixed reference mesh and a time dependent embedding into physical space, subject to shape regularity constraints [18, 19]. The crucial difference is that in standard ALE methods the mesh motion is prescribed by a deterministic algorithm, often to equidistribute discretization error, and the mesh is not part of the dynamical system. In DLR the embedding variables  $x(n)$  are integrated over quantum–mechanically; one may regard the scheme as a “quantum ALE” version of lattice field theory. At a continuum level, one may also view the geometry sector as an “elastic–coordinate” field theory in which one integrates over maps  $x : M \rightarrow \mathbb{R}^d$  on a fixed reference space  $M$ , with a local energy depending on  $\partial x$  and with some nondegeneracy conditions.

These comparisons place DLR as a conservative middle ground between rigid hypercubic lattices and more radical fluctuating–topology approaches: the topology and constructive–QFT structure of Wilson’s lattice theory are retained, while an intrinsic, dynamically fluctuating geometry is used to restore global Euclidean symmetry and, potentially, to reduce lattice artefacts.

## 2 Geometry of the dynamical lattice regulator

### 2.1 Abstract lattice, fields, and embedding

Let  $d \geq 2$ . We take as abstract lattice either

- the infinite hypercubic lattice  $\Lambda = \mathbb{Z}^d$ , or
- for finite volume simulations, the discrete torus

$$\Lambda = \{0, \dots, L_1 - 1\} \times \dots \times \{0, \dots, L_d - 1\}, \quad (2.1)$$

with periodic identification in each direction.

In either case we denote by  $\hat{\mu}$ , for  $\mu = 1, \dots, d$ , the unit vectors in the coordinate directions and write  $n + \hat{\mu}$  for the nearest neighbour of  $n$  in direction  $\mu$ .

We fix a compact gauge group  $G$ . Gauge fields are represented by link variables

$$U_\mu(n) \in G \quad (2.2)$$



attached to the oriented link  $(n, n + \hat{\mu})$ . Matter fields are collected in a variable  $\Phi(n)$  living in some representation space of  $G$ . Examples are  $\Phi(n) \in \mathbb{R}$  for a real scalar field,  $\Phi(n) \in \mathbb{C}^N$  for a complex scalar multiplet, and a spinor representation for fermions. The collection of all  $U_\mu(n)$  and  $\Phi(n)$  on  $\Lambda$  forms the usual field content of a lattice gauge theory.

The new ingredient is a geometry field

$$x : \Lambda \rightarrow \mathbb{R}^d, \quad (2.3)$$

which assigns to each abstract site  $n \in \Lambda$  a point  $x(n) \in \mathbb{R}^d$  in physical Euclidean space. In the torus formulation one instead takes  $x(n) \in \mathbb{T}^d$  and works with the shortest distance representative of coordinate differences; the local constructions in what follows are unchanged.

It is often convenient to regard the geometry field  $x$  as part of an *extended* field multiplet, alongside the gauge and matter fields:

$$(x, U, \Phi) \in (\mathbb{R}^d)^\Lambda \times G^{\text{links}} \times \mathcal{F}_{\text{matter}}. \quad (2.4)$$

In this viewpoint DLR is simply a local lattice field theory with additional scalar degrees of freedom  $x_\mu(n)$  and a special pattern of couplings. This extended-field formulation will be crucial in Section 4, where reflection positivity is established by letting the Osterwalder–Schrader reflection act on the indices  $n$  and treating  $x$  on the same footing as the other fields.

## 2.2 Local Euclidean geometry and admissible embeddings

We spell out the local Euclidean geometry induced by an embedding  $x : \Lambda \rightarrow \mathbb{R}^d$  of the abstract lattice and formulate our admissibility conditions. Throughout this subsection we work on  $\mathbb{R}^d$ ; the periodic (torus) version will be discussed in Section 2.4.

Given  $x : \Lambda \rightarrow \mathbb{R}^d$  and a site  $n \in \Lambda$ , we define the (forward and backward) *edge vectors*

$$e_\mu^\pm(n) = x(n \pm \hat{\mu}) - x(n) \in \mathbb{R}^d, \quad \mu = 1, \dots, d, \quad (2.5)$$

where  $\hat{\mu}$  denotes the unit vector in the  $\mu$ -th lattice direction. We may write the forward vectors simply as  $e_\mu(n) = e_\mu^+(n)$ . We then define the (advanced and retarded) *frame matrices*

$$E(n) = [e_1(n) \ e_2(n) \ \dots \ e_d(n)] \in \mathbb{R}^{d \times d}, \quad (2.6)$$

and

$$E^\theta(n) = [e_1^-(n) \ e_2(n) \ \dots \ e_d(n)] \in \mathbb{R}^{d \times d}. \quad (2.7)$$

The associated (advanced) *Gram matrix* (or local metric) and *local volume* are then

$$g(n) = E(n)^\top E(n), \quad V(n) = |\det E(n)| = \sqrt{\det g(n)}. \quad (2.8)$$

In  $d = 2$ ,  $V(n)$  is the (unsigned) area of the outgoing edge parallelogram at  $n$ ; for a non-affine embedded plaquette it need not coincide with the Euclidean area of the quadrilateral cell. The components of  $g(n)$  are  $g_{\mu\nu} = e_\mu(n) \cdot e_\nu(n)$ . Whenever  $g(n)$  is positive definite we denote the components of its inverse by  $g^{\mu\nu}(n)$ .

We restrict attention to embeddings for which each pair  $E(n)$  and  $E^\theta(n)$  is uniformly non-degenerate and uniformly shape regular, in a way that is stable under global proper Euclidean motions. A convenient local formulation is the following.

**Definition 2.1.** Fix dimensionless constants  $C_\ell \geq 1$  and  $c_V \leq 1$ . Then for a parameter  $a > 0$ , an embedding  $x : \Lambda \rightarrow \mathbb{R}^d$  is called *a-admissible* if for every  $n \in \Lambda$  we have

$$|e_\mu(n)| \leq C_\ell a \quad (\mu = 1, \dots, d), \quad \min\{\det E(n), -\det E^\theta(n)\} \geq c_V a^d. \quad (2.9)$$

We denote by  $\hat{\mathcal{X}}_{\text{adm}}(a) \subset (\mathbb{R}^d)^\Lambda$  the set of all *a*-admissible embeddings.

Conditions (2.9) are local (they can be checked independently at each site) and invariant under global translations and proper rotations  $x \mapsto Rx + b$  with  $R \in \text{SO}(d)$  and  $b \in \mathbb{R}^d$ . Note, however, that the lower bound on the oriented volumes  $\det E(n)$  and  $-\det E^\theta(n)$  selects an orientation sector: under an improper rotation  $R \in \text{O}(d) \setminus \text{SO}(d)$  one has

$$\det(RE(n)) = \det(R) \det E(n) = -\det E(n), \quad (2.10)$$

and the same behavior for  $\det E^\theta(n)$ , so  $\hat{\mathcal{X}}_{\text{adm}}$  is not invariant under the full Euclidean group  $\text{E}(d) = \text{O}(d) \times \mathbb{R}^d$  but only under the special Euclidean subgroup  $\text{SE}(d) = \text{SO}(d) \times \mathbb{R}^d$ . This point is discussed further in §3.2.

**Remark 2.2.** For  $x \in \hat{\mathcal{X}}_{\text{adm}}(a)$  introduce the dimensionless embedding  $y(n) = a^{-1}x(n)$ . Then in terms of  $y$ , the admissibility conditions (2.9) become *a*-independent bounds, meaning that  $\hat{\mathcal{X}}_{\text{adm}}(a)$  is a simple rescaling of  $\hat{\mathcal{X}}_{\text{adm}}(1)$ .

The next lemma records the basic geometric consequences of admissibility.

**Lemma 2.3.** Let  $x \in \hat{\mathcal{X}}_{\text{adm}}(a)$  be an admissible embedding in the sense of Definition 2.1. Then there exist a constant  $C^*$ , depending only on  $C_\ell$ ,  $c_V$ , and the dimension  $d$ , such that

$$\|E(n)^{-1}\| + \|E^\theta(n)^{-1}\| \leq C^* a^{-1} \quad \text{for all } n. \quad (2.11)$$

*Proof.* Fix  $n$ . Write the rescaled frames  $\tilde{E} = a^{-1}E(n)$  and  $\tilde{E}^\theta = a^{-1}E^\theta(n)$ . Then the defining bounds for admissibility (edge lengths  $\sim a$  and oriented volumes  $\sim a^d$ ) become uniform bounds for  $\tilde{E}$  and  $\tilde{E}^\theta$  at scale  $a = 1$ . The set of all such  $\tilde{E}$  is closed and bounded in the space of invertible matrices with  $\det \tilde{E}$  bounded away from 0, hence compact. The continuous map  $A \mapsto \|A^{-1}\|$  attains a finite maximum on this set, say  $\|\tilde{E}^{-1}\| \leq C$  and  $\|(\tilde{E}^\theta)^{-1}\| \leq C$  with  $C$  depending only on  $(C_\ell, c_V, d)$ . Finally, we note

$$E(n)^{-1} = (a\tilde{E})^{-1} = a^{-1}\tilde{E}^{-1}, \quad (E^\theta(n))^{-1} = a^{-1}(\tilde{E}^\theta)^{-1}, \quad (2.12)$$

establishing the lemma with  $C^* = 2C$ . □

The content of Lemma 2.3 is that the eigenvalues of the local metrics are uniformly bounded above and below away from 0. In numerical-analysis language this is a standard “shape-regularity” condition: the local affine cells determined by the corner frames cannot be arbitrarily skinny or flat. In particular, (2.9) excludes local collapses of volume and guarantees that the embedding  $x : \Lambda \rightarrow \mathbb{R}^d$  is everywhere locally an immersion with controlled condition number. Global properties such as non-self-intersection will be enforced by restricting  $x$  to a suitable admissible component in Definition 2.5 and, if desired, by adding further constraints as discussed in the next remark.

**Remark 2.4.** The formulation in Definition 2.1 is deliberately minimal: it is stable under global Euclidean transformations and sufficient for the geometric estimates in Lemma 2.3. In concrete implementations it is often convenient to replace or strengthen (2.9) by more classical mesh conditions. We briefly record a few equivalent or stronger variants.

(A1) *Edge length lower bound.* For each  $\mu = 1, \dots, d$ , we require

$$|e_\mu(n)| \geq c_\ell a. \quad (2.13)$$

This prevents local “collapses” of edges.

(A2) *Angle bounds.* For all  $\mu \neq \nu$  we require

$$\frac{|e_\mu(n) \cdot e_\nu(n)|}{|e_\mu(n)||e_\nu(n)|} \leq \cos \varepsilon_0. \quad (2.14)$$

That is, the angle between any pair of edges is bounded away from 0 and  $\pi$ .

(A3) *All-corner volume bounds.* One may strengthen the determinant condition in (2.9) by requiring nondegeneracy of *all*  $2^d$  corner frames incident to  $n$ . Concretely, for each site  $n$  and each choice of forward/backward directions  $\sigma \in \{\pm 1\}^d$ , let  $E^\sigma(n)$  be the  $d \times d$  “corner frame” obtained by taking, in each coordinate direction  $\mu$ , the edge from  $n$  to  $n + \sigma_\mu \hat{\mu}$ . Then impose the uniform oriented-volume bound

$$\min_{\sigma \in \{\pm 1\}^d} \left( \prod_{\mu=1}^d \sigma_\mu \right) \det E^\sigma(n) \geq c_V a^d \quad \text{for all } n \in \Lambda. \quad (2.15)$$

This rules out fold-overs at any corner and is convenient when actions involve mixed forward/backward stencils in several directions.

(A4) *Cell convexity.* In addition to local nondegeneracy of the edge frame, one may require each elementary cell to be *geometrically convex* in  $\mathbb{R}^d$ . For instance, in  $d = 2$ , the elementary cell  $Q(n)$  at  $n$  is the quadrilateral with vertices

$$x(n), \quad x(n + e_1), \quad x(n + e_1 + e_2), \quad x(n + e_2). \quad (2.16)$$

(A5) *Cell shape regularity.* If desired, one may impose a standard finite–element shape–regularity assumption on the embedded cells: taking the  $2d$  case for example, each quadrilateral image is required to be convex and to have uniformly bounded chunkiness parameter  $h_Q/\rho_Q$  (diameter over inradius), uniformly in the lattice and in the configuration. Equivalently, one may enforce a uniform lower bound on all interior angles together with a uniform bound on edge–length ratios; any of the standard equivalent criteria may be used.

(A6) *Global embedding / non–self–intersection.* The conditions above control the local geometry but do not, by themselves, preclude global self–intersections of the mesh. In simulations it is often convenient to restrict to embeddings that are globally injective and avoid edge crossings, for example by imposing a uniform separation condition

$$|x(n) - x(m)| \geq \delta_{\text{sep}} a \quad \text{for all } n \neq m. \quad (2.17)$$

This ensures that the dynamical mesh remains a controlled distortion of the reference lattice without changes in combinatorics or global foldings.

In practice, conditions such as cell convexity and uniform cell shape regularity are effective guards against self–intersection: a mesh made of embedded convex cells cannot “fold” locally, and when combined with a mild global separation condition that is occasionally enforced, they prevent distant parts of the mesh from passing through one another under local Monte Carlo updates. Thus convexity constraints serve as a computationally cheap proxy for global non–self–intersection checks in many settings.

The set  $\hat{\mathcal{X}}_{\text{adm}}(a)$  of admissible embeddings typically has several connected components, corresponding for instance to different global windings on a torus. For the purposes of this paper we focus on the component that contains the regular hypercubic embedding.

**Definition 2.5.** Let  $x_0(n) = an$  be the regular embedding at scale  $a > 0$ . The *principal admissible component*  $\mathcal{X}_{\text{adm}}(a)$  is the connected component of  $\hat{\mathcal{X}}_{\text{adm}}(a)$  containing  $x_0$ , i.e.,

$$\mathcal{X}_{\text{adm}}(a) = \{x \in \hat{\mathcal{X}}_{\text{adm}}(a) : x \text{ can be connected to } x_0 \text{ by a continuous path inside } \hat{\mathcal{X}}_{\text{adm}}(a)\}.$$

If the scale  $a$  is to be irrelevant or inferred from the context, which will be the case for the most of this paper, we may simply write  $\mathcal{X}_{\text{adm}}$  for  $\mathcal{X}_{\text{adm}}(a)$ .

Working in  $\mathcal{X}_{\text{adm}}$  ensures that the dynamical mesh remains a controlled distortion of the regular hypercubic grid: shape regularity is enforced uniformly by Lemma 2.3, and no topological defects (such as changes in the combinatorial structure or global self-intersections) are introduced by the fluctuations of  $x$ . This sector is the natural setting for both the perturbative Symanzik analysis and the nonperturbative reflection positivity arguments that follow.

### 2.3 Geometry measure and dynamics

The geometry field  $x : \Lambda \rightarrow \mathbb{R}^d$  is treated as a genuine dynamical degree of freedom of the regulator. In the Euclidean functional integral we integrate  $x$  over the principal admissible component  $\mathcal{X}_{\text{adm}} \subset (\mathbb{R}^d)^\Lambda$  introduced in Definition 2.5. The corresponding geometry measure is of the form

$$d\mu_x(x) = \frac{1}{Z_x} \exp(-S_x[x]) Dx, \quad Dx = \prod_{n \in \Lambda} d^d x(n), \quad (2.18)$$

where  $S_x[x]$  is local and depends on  $x$  only through Euclidean invariants of the local edge data (hence is  $\text{SE}(d)$ -covariant on  $\mathcal{X}_{\text{adm}}$ ), and  $Z_x$  is the corresponding normalisation factor. The hard admissibility constraint is implemented by restricting the domain of integration to  $\mathcal{X}_{\text{adm}}$ ; we do *not* insert a separate indicator function into the integrand.

Throughout we take the geometry integration measure to be the flat product Lebesgue measure  $Dx = \prod_{n \in \Lambda} d^d x(n)$  restricted to  $\mathcal{X}_{\text{adm}}$ , optionally reweighted by  $\exp(-S_x[x])$ . This is the natural choice in the embedding-field formulation:  $x(n)$  are fundamental variables and the theory is not intended to be reparametrization-invariant (unlike lattice quantum gravity). Alternative “geometric” measures (e.g. inserting local factors built from  $\sqrt{\det g(n)}$ ) would amount to a specific local reweighting of configurations and can be viewed as part of the choice of  $S_x$  or local counterterms. We keep the flat measure to preserve the manifest global shift symmetry  $x \mapsto x + b$  and to keep the regulator definition transparent.

**Minimal choice.** The conceptually simplest choice is the “minimal” geometry action

$$S_x^{\text{min}}[x] \equiv 0, \quad (2.19)$$

so that  $d\mu_x$  is just the restriction of the flat product measure  $Dx$  to  $\mathcal{X}_{\text{adm}}$ . The admissibility conditions from Definition 2.1 and Remark 2.4 then appear as hard walls in configuration space: any proposed configuration outside  $\mathcal{X}_{\text{adm}}$  is assigned infinite action and zero measure. Even in this minimal setting the geometry does not behave as a collection of non-interacting free variables. Because  $\mathcal{X}_{\text{adm}}$  is a nontrivial subset of  $(\mathbb{R}^d)^\Lambda$ , the restriction  $x \in \mathcal{X}_{\text{adm}}$  induces effective interactions

between neighbouring sites via purely entropic effects: the volume in configuration space available to a site  $x(n)$  depends on the positions of its neighbours through the local admissibility constraints.

In  $d = 2$  our exploratory simulations suggest that the minimal measure  $S_x^{\min} \equiv 0$  together with the hard walls can already yield a stable, nondegenerate ensemble. In higher dimensions, especially in  $d = 4$ , this is *not* guaranteed: entropic effects alone may admit phases with long-range geometric correlations or crumpling/roughening phenomena in which the lattice spacing ceases to define a clean regulator scale. For four-dimensional applications we therefore expect that an explicit stiffness term (for instance (2.21) or variants) will be necessary in practice to remain in a short-range geometry regime (SR), that will be formulated below.

**Local  $E(d)$ -invariant penalty terms.** For practical simulations it is often advantageous to supplement the hard admissibility constraints by soft, local penalties which keep the mesh away from the boundary of  $\mathcal{X}_{\text{adm}}$  and disfavour excessively distorted cells. A general geometry action of this form can be written as a sum of local terms

$$S_x[x] = \sum_{n \in \Lambda} s_x(g(n), g(n)^{-1}, V(n)), \quad (2.20)$$

where  $s_x$  is a scalar function of the local metric and volume at site  $n$ , and  $g(n), V(n)$  are the Gram matrix and volume from Section 2.2. Because  $g(n)$  and  $V(n)$  are built from the edge vectors  $e_\mu(n)$  via Euclidean inner products, any such  $s_x$  is automatically invariant under global Euclidean transformations  $x \mapsto Rx + b$ ; see Section 3.2.

A particularly transparent class of such penalties are “spring” terms that keep the local metric  $g(n)$  close to a prescribed target. For instance, fixing a target length scale  $a > 0$ , one may penalise deviations from the Euclidean reference metric  $a^2 I$  by

$$S_{\text{spr}}[x] = \alpha \sum_{n \in \Lambda} \sum_{\mu, \nu} (e_\mu(n) \cdot e_\nu(n) - a^2 \delta_{\mu\nu})^2. \quad (2.21)$$

The diagonal terms  $\mu = \nu$  act as *edge springs*, keeping  $|e_\mu(n)|$  near  $a$ , while the off-diagonal terms  $\mu \neq \nu$  act as *angle springs*, favouring near-orthogonality of neighbouring edges. This is only an illustrative example: by replacing  $a^2 I$  with an arbitrary positive definite reference matrix, or by applying the same “soft constraint” philosophy to other local invariants, such as  $V(n)$  and the eigenvalues of  $g(n)$ , one obtains many further  $E(d)$ -invariant local choices, all encompassed by the general form (2.20).

In practice the coupling  $\alpha$  is taken small enough that the geometry remains a mild fluctuation around the regular lattice, but large enough to discourage excursions toward highly distorted cells or toward the boundary of  $\mathcal{X}_{\text{adm}}$ .

Penalties of the form (2.21) are designed to suppress long-wavelength distortions of the local frame and thus to promote a massive (finite-correlation-length) geometry sector once the global  $SE(d)$  zero modes are fixed/quotiented. In the language of Section 4.3, such choices are intended to place the geometry in a regime compatible with the short-range geometry hypothesis (SR).

**Universality and the role of  $S_x$ .** From the viewpoint of effective field theory, different choices of the geometry action  $S_x$  define different microscopic regulators, but as long as  $S_x$  is local,  $E(d)$ -invariant, and compatible with the admissibility conditions, they are expected to lie in the same universality class. One may also view the choice of  $S_x$  (more precisely, the local weight  $e^{-S_x[x]}$  together with the admissible-set restriction) as selecting an effective *submanifold measure* on the space of embedded lattices inside the continuum configuration space: it specifies how

the enlarged, finite-dimensional family of fields induced by the embedding  $x$  is sampled. This reweighting is not required by an exact local redundancy, but changing it (within the same locality and symmetry class) is expected to affect the continuum limit only through symmetry-allowed local counterterms. Integrating out the geometry field induces local, higher-dimensional operators in the effective action for the gauge and matter fields; these operators are constrained by gauge invariance, Euclidean invariance, and reflection positivity, and are therefore irrelevant in the renormalisation-group sense in the continuum limit. We will see an explicit perturbative example of this mechanism in the Symanzik expansion for a scalar theory in §4.4.

**Global zero modes versus local twisting.** The embedding variables  $x(n)$  enjoy an exact global  $SE(d)$  symmetry,  $x(n) \mapsto Rx(n) + b$ , acting uniformly on all sites. In infinite volume this produces non-normalisable zero modes, and in finite volume an irrelevant overall group-volume factor. In practice one therefore fixes or quotients these global modes by a convenient convention, e.g., pinning the centre of mass and fixing the orientation of a chosen local frame. This step does *not* affect local observables and is entirely analogous to removing rigid-motion zero modes in molecular simulations.

The practically relevant question is not whether the regulator is *formally*  $SE(d)$ -covariant (it is, by construction), but how this covariance is *realised* in the ensemble in a way compatible with universality. Our Symanzik discussion is conditional on the short-range geometry hypothesis (SR); under this assumption, integrating out  $x$  produces only local, irrelevant corrections in the effective action. Within this regime, rigid global motions cannot implement  $SE(d)$  covariance at the level of local probes (they carry no local geometric information), and any attempt to enforce isotropy through genuinely long-range geometric modes would violate (SR) and could in principle change the universality class. Thus, in the intended operating regime,  $SE(d)$  covariance that is *felt locally* must come from the *local* embedding fluctuations—twisting, shearing, and local reorientation from cell to cell—which average short distance observables over many local frames while keeping the underlying hypercubic connectivity fixed.

**Monte Carlo dynamics.** In numerical simulations the geometry field  $x$  is updated by local Metropolis moves of the form  $x(n) \rightarrow x(n) + \delta x$  with  $\delta x$  drawn from a symmetric proposal distribution, followed by an admissibility check at the sites affected by the move and an acceptance test based on the local change in  $S_x[x]$  and in the field action. Because  $S_x$  is local, the acceptance probability can be evaluated from a uniformly bounded neighbourhood of  $n$ , and the resulting Markov chain is manifestly local on the abstract lattice. A detailed description of the update scheme and its ergodicity properties is deferred to the numerics section §5.

From an algorithmic standpoint, the dynamical geometry sector adds only a mild overhead compared to standard lattice gauge theory. A local proposal  $x(n) \mapsto x(n) + \delta x$  affects only the finite set of terms in  $S_x$  and in  $S_{\text{fields}}$  that involve  $n$  and its nearest neighbours, so both the admissibility check and the Metropolis acceptance ratio can be evaluated in  $O(1)$  work per proposal, with a constant depending only on the dimension and the chosen locality range, not on the lattice volume. A full “sweep” of geometry updates therefore costs  $O(|\Lambda|)$ , just as in standard LGT. In practice the geometry update can be interleaved with the usual gauge and matter updates (or combined in a hybrid scheme), and the method remains compatible with existing locality-based implementations; the principal new ingredient is the additional bookkeeping of the local geometric data needed to evaluate the affected action terms.

## 2.4 Torus version and periodic implementation

For most analytical questions, it is convenient to regard the dynamical lattice as embedded into the full Euclidean space  $\mathbb{R}^d$ . In numerical simulations, however, one typically works at finite volume with periodic boundary conditions, i.e., on a  $d$ -dimensional discrete torus.

There are two equivalent ways to formulate this periodic setting:

- (i) *Intrinsic formulation on the discrete torus.* Fix an integer  $N \geq 1$  and set

$$\Lambda = (\mathbb{Z}/N\mathbb{Z})^d, \quad (2.22)$$

viewed as a periodic hypercubic lattice. The geometry field is a map

$$x : \Lambda \rightarrow \mathbb{T}^d = (\mathbb{R}/L\mathbb{Z})^d \quad (2.23)$$

for some physical period  $L > 0$ . Differences  $x(n + \hat{\mu}) - x(n)$  are interpreted modulo  $L\mathbb{Z}^d$ , and the edge vectors  $e_\mu(n)$  are chosen as the unique representatives of these differences in a fixed fundamental domain of  $\mathbb{T}^d$  (for instance  $(-L/2, L/2]^d$ ). Local geometric quantities are then defined from these edge vectors exactly as in the  $\mathbb{R}^d$  setting.

- (ii) *Periodic formulation on  $\mathbb{Z}^d$ .* Alternatively, one may take the index set to be the infinite lattice

$$\Lambda = \mathbb{Z}^d, \quad (2.24)$$

and work with an embedding  $x : \Lambda \rightarrow \mathbb{R}^d$  satisfying the quasi-periodicity condition

$$x(n + N\hat{\mu}) = x(n) + L\hat{e}_\mu, \quad \mu = 1, \dots, d. \quad (2.25)$$

All geometric quantities are computed from  $x$  exactly as before, while observables and the action are invariant under global shifts  $x \mapsto x + Lk$  with  $k \in \mathbb{Z}^d$ . Passing to the quotient by the relations (2.25) recovers the intrinsic discrete-torus description in (i).

In both formulations the local admissibility conditions are imposed on the edge vectors  $e_\mu(n)$ , and the principal admissible component  $\mathcal{X}_{\text{adm}}$  is understood modulo periodicity. Global non-self-intersection is likewise interpreted in the periodic sense: cells may wrap around the torus, but configurations in which large portions of the mesh fold back and concentrate in a small region are excluded by the same local shape regularity and volume constraints as in the  $\mathbb{R}^d$  setting.

The passage from  $\mathbb{R}^d$  to  $\mathbb{T}^d$  does not affect any of the local arguments in this paper. In particular, the construction of the geometry measure  $d\mu_x$  and of the field actions remains unchanged, and the analysis of Euclidean invariance and reflection positivity is carried out on  $\mathbb{R}^d$  and then transferred to the periodic case in the standard way. For the Monte Carlo implementation we restrict to a finite periodic lattice and update the geometry field subject to these periodic admissibility constraints; the details of the algorithm are deferred to the numerical section.

## 3 Field actions and symmetries on a dynamical lattice

### 3.1 Configuration space and full action

We summarise the full configuration space and the action of the dynamical lattice regulator. The basic kinematical variables are:

- a geometry field  $x : \Lambda \rightarrow \mathbb{R}^d$ , constrained to take values in the principal admissible component  $\mathcal{X}_{\text{adm}} \subset (\mathbb{R}^d)^\Lambda$  introduced in Section 2.2;
- gauge link variables  $U_\mu(n) \in G$  attached to each oriented edge  $(n, \mu)$  of the abstract hypercubic lattice  $\Lambda$ ;
- matter fields  $\Phi(n)$  (scalars, spinors, etc.) living on the sites  $n \in \Lambda$ .

We denote the full configuration collectively by  $(x, U, \Phi)$ . The geometry degrees of freedom  $x$  are governed by a local action  $S_x[x]$  built from Euclidean invariants of the embedding data as in §2.3, while the gauge and matter fields are coupled to  $x$  through a local field action  $S_{\text{fields}}[x, U, \Phi]$ . The total action is

$$S[x, U, \Phi] = S_x[x] + S_{\text{fields}}[x, U, \Phi]. \quad (3.1)$$

For complete precision one first defines the functional integral in finite volume, for instance on a time-open cylinder  $\Lambda_{T,L} \subset \mathbb{Z}^d$ , with the first lattice direction singled out as index time, where all measures are ordinary finite products. The infinite-lattice notation used below is then understood as the limit  $\Lambda_{T,L} \nearrow \mathbb{Z}^d$  on local observables. Global translation/rotation zero modes of  $x$  may be fixed (or quotiented) in finite volume; this does not affect the local structure of the actions below nor the reflection positivity statements proved later.

Thus the Euclidean functional integral is defined formally by

$$Z = \int_{\mathcal{X}_{\text{adm}}} Dx \int DU \int D\Phi \exp(-S_x[x] - S_{\text{fields}}[x, U, \Phi]), \quad (3.2)$$

where  $Dx$  is the flat measure in  $\mathcal{X}_{\text{adm}}$ ,  $DU$  is the product Haar measure over link variables, and  $D\Phi$  is the standard product measure over matter fields, which is the Lebesgue measure for bosons and the usual Grassmann measure for fermions.

We present a representative class of gauge and matter actions on a dynamical mesh. In all cases the fields live on the abstract lattice  $\Lambda$ , and the interactions have the usual nearest neighbour stencil, with couplings dressed by local geometry dependent weights. For later Osterwalder–Schrader (OS) reflection-positivity arguments, one subtlety is important: the local metric and volume constructed from a *forward* corner frame are intrinsically biased with respect to the time direction. Rather than modifying the finite-difference stencils, we remove this bias by *action averaging*: we define two local geometric dressings, exchanged by the OS reflection, and average the resulting actions. This produces a manifestly reflection invariant field action while preserving locality and gauge invariance.

**Signed directions and the induced reflection on directions.** Let

$$\Delta = \{\pm 1, \dots, \pm d\}, \quad (3.3)$$

denote the set of signed coordinate directions, and write  $\hat{\mu} \in \mathbb{Z}^d$  for the corresponding unit vectors, so that  $\widehat{-\mu} = -\hat{\mu}$ . We single out  $\mu = 1$  as the index-time direction, and define the time-reflection  $\theta$  on directions by

$$\theta(\pm 1) = \mp 1, \quad \theta(\pm i) = \pm i \quad (i = 2, \dots, d), \quad \text{equivalently} \quad \theta(\hat{\mu}) = \widehat{\theta(\mu)}. \quad (3.4)$$

For  $\mu \in \Delta$  define the oriented edge vectors and gauge links by

$$e_\mu(n) = x(n + \hat{\mu}) - x(n), \quad U_{-\mu}(n) = U_\mu(n - \hat{\mu})^{-1}. \quad (3.5)$$



Thus  $U_\mu(n)$  always lives on the oriented link  $n \rightarrow n + \hat{\mu}$ , for both positive and negative directions. With this convention, we can write (2.5) now as  $e_\mu^\pm(n) = e_{\pm\mu}(n)$ .

**Prototype actions and  $\theta$ -averaging.** Recall from (2.6)-(2.8) the advanced and retarded frames  $E(n)$  and  $E^\theta(n)$ , as well as the local metric  $g(n)$  and volume  $V(n)$  computed from  $E(n)$ . We first define ‘‘prototype’’ field actions  $S^\circ[x, U, \Phi]$  by coupling the usual nearest-neighbour stencils to  $g$  and  $V$ . To remove the forward-time bias, we then define the  $\theta$ -partner action  $S^\theta[x, U, \Phi]$  by the same formulas but with every occurrence of a direction index  $\mu$  replaced by  $\theta(\mu)$  and with the corner frame replaced by its  $\theta$ -version. Averaging the two yields the field action

$$S_{\text{fields}}[x, U, \Phi] = \frac{1}{2}(S^\circ[x, U, \Phi] + S^\theta[x, U, \Phi]). \quad (3.6)$$

Notice that since  $g$  and  $V$  depend on  $E$ , to get  $S^\theta$ , any occurrences of  $g$  and  $V$  in  $S^\circ$  should be replaced by  $g^\theta$  and  $V^\theta$ , that are computed from  $E^\theta$  instead of  $E$ . By construction this preserves locality and gauge invariance, and it is compatible with the OS reflection  $\Theta$  introduced later.

More generally, one may analogously symmetrize with respect to reflections in any coordinate direction (or build the action directly from such symmetrized geometric data), which reduces directional bias and makes the couplings more isotropic with respect to the lattice axes.

**Scalar fields.** Let  $\phi : \Lambda \rightarrow \mathbb{C}^m$  be a complex scalar multiplet transforming in some unitary representation of  $G$ . For  $\mu \in \Delta$  define the gauge-covariant signed forward difference

$$\nabla_\mu \phi(n) = \frac{U_\mu(n) \phi(n + \hat{\mu}) - \phi(n)}{|e_\mu(n)|}. \quad (3.7)$$

The prototype scalar kinetic and potential contributions are

$$S_{\phi, \text{kin}}^\circ[x, \phi, U] = \frac{1}{2} \sum_{n \in \Lambda} V(n) \sum_{\mu, \nu=1}^d (g(n)^{-1})^{\mu\nu} \langle \nabla_\mu \phi(n), \nabla_\nu \phi(n) \rangle, \quad (3.8)$$

$$S_{\phi, \text{pot}}^\circ[x, \phi] = \sum_{n \in \Lambda} V(n) W_{\text{loc}}(\phi(n)), \quad (3.9)$$

where  $\langle a, b \rangle = a^\dagger b$  and  $W_{\text{loc}}$  is a local gauge-invariant potential such as

$$W_{\text{loc}}(\phi) = \frac{m_0^2}{2} \phi^\dagger \phi + \frac{\lambda_0}{4!} (\phi^\dagger \phi)^2. \quad (3.10)$$

We define the prototype scalar action  $S_\phi^\circ = S_{\phi, \text{kin}}^\circ + S_{\phi, \text{pot}}^\circ$  and then set

$$S_\phi[x, \phi, U] = \frac{1}{2} (S_\phi^\circ[x, \phi, U] + S_\phi^\theta[x, \phi, U]). \quad (3.11)$$

To reiterate the definition of  $S_\phi^\theta$ , it is defined by replacing  $(g, V)$  with  $(g^\theta, V^\theta)$  and applying  $\mu \mapsto \theta(\mu)$  to the direction labels appearing in (3.8), so that only the time-direction differences are reversed. On the regular embedding  $x(n) = an$  one has  $E(n) = aI$  and  $E^\theta(n) = aR_\theta$  with  $R_\theta = \text{diag}(-1, 1, \dots, 1)$ . In particular  $g(n) = E(n)^\top E(n) = a^2 I$  and  $g^\theta(n) = (E^\theta(n))^\top E^\theta(n) = a^2 I$ . Hence the  $\theta$ -averaged scalar action reduces to the standard hypercubic action.

One may alternatively use a centered covariant difference or higher-order stencils to reduce cutoff effects. For example, a nearest-neighbour centered difference can be defined by

$$\nabla_\mu^{\text{sym}} \phi(n) = \frac{U_\mu(n) \phi(n + \hat{\mu}) - U_{-\mu}(n) \phi(n - \hat{\mu})}{|e_\mu(n)| + |e_{-\mu}(n)|}, \quad (3.12)$$

though we will not pursue such refinements in the present work.

**Gauge fields.** For the gauge sector we use a Wilson-type plaquette action coupled to the embedding through local positive weights. For  $\mu, \nu \in \Delta$  define the oriented plaquette holonomy by the uniform formula

$$U_{\mu\nu}(n) = U_\mu(n) U_\nu(n + \hat{\mu}) U_\mu(n + \hat{\nu})^{-1} U_\nu(n)^{-1}. \quad (3.13)$$

For  $\mu, \nu > 0$  this agrees with the usual plaquette; for  $\mu < 0$  it represents the oppositely oriented plaquette based at  $n$ , encoded using (3.5). The prototype gauge action is

$$S_g^\circ[x, U] = \frac{\beta}{N} \sum_{n \in \Lambda} \sum_{1 \leq \mu < \nu \leq d} w^{\mu\nu}(n; x) \Re \text{tr}(I - U_{\mu\nu}(n)), \quad (3.14)$$

where the weight  $w^{\mu\nu}(n; x) > 0$  depends on the embedding only through local Euclidean invariants built from  $(g(n), V(n))$ , or equivalently from  $E(n)$ . Two natural choices are

$$w^{\mu\nu}(n; x) = V(n) \left( (g(n)^{-1})^{\mu\mu} (g(n)^{-1})^{\nu\nu} - [(g(n)^{-1})^{\mu\nu}]^2 \right), \quad (3.15)$$

and

$$w^{\mu\nu}(n; x) = \frac{V(n)}{A_{\mu\nu}(n)^2}, \quad A_{\mu\nu}(n) = |e_\mu(n) \wedge e_\nu(n)|, \quad (3.16)$$

where in (3.16) the signed edges  $e_\mu(n)$  are given by (3.5). The coefficients in (3.15) are precisely those arising from the contraction  $\sqrt{g} F_{\mu\nu} F^{\mu\nu}$  with the inverse metric in coordinate components. On a regular embedding  $x(n) = an$ , both weights reduce to a constant  $w_{\mu\nu} \equiv a^{d-4}$ , so (3.14) reduces (after absorbing this constant into  $\beta$ ) to the standard Wilson plaquette action.

We then define the averaged gauge action by

$$S_g[x, U] = \frac{1}{2} \left( S_g^\circ[x, U] + S_g^\theta[x, U] \right), \quad (3.17)$$

Concretely, applying  $\mu \mapsto \theta(\mu)$  inside the plaquette (3.13) reverses precisely the time-oriented plaquettes, so that the  $\theta$ -partner couples the  $E^\theta$ -based weights to the corresponding backward-time plaquettes at the same basepoint  $n$ .

**Fermions.** Fermionic actions on a dynamical lattice can be constructed in close analogy with the standard hypercubic case, with the difference that the discrete Dirac operator must be built from the local geometry induced by the embedding  $x$ . Let  $\psi(n)$  and  $\bar{\psi}(n)$  be lattice Dirac spinors (Grassmann fields) in a representation of  $G$ . Fix Euclidean gamma matrices  $\{\gamma_a\}_{a=1}^d$  with  $\{\gamma_a, \gamma_b\} = 2\delta_{ab}$ , and define

$$\Gamma_\mu(n) = \sum_{a=1}^d \gamma_a (E(n)^{-1})_{a\mu}, \quad \Gamma_\mu^\theta(n) = \sum_{a=1}^d \gamma_a (E^\theta(n)^{-1})_{a\mu}. \quad (3.18)$$

The prototype naive Dirac operator is

$$(D_{\text{naive}}^\circ \psi)(n) = \frac{1}{2} \sum_{\mu=1}^d \left( \Gamma_\mu(n) U_\mu(n) \psi(n + \hat{\mu}) - \Gamma_\mu^\theta(n) U_{-\mu}(n) \psi(n - \hat{\mu}) \right), \quad (3.19)$$

and the corresponding fermion action is

$$S_f^\circ[x, \bar{\psi}, \psi, U] = \sum_{n \in \Lambda} V(n) \bar{\psi}(n) (D_{\text{naive}}^\circ \psi)(n). \quad (3.20)$$

We define the  $\theta$ -partner by the same stencil but with the advanced/retarded geometric data interchanged, i.e.

$$(D_{\text{naive}}^\theta \psi)(n) = \frac{1}{2} \sum_{\mu=1}^d \left( \Gamma_\mu^\theta(n) U_\mu(n) \psi(n + \hat{\mu}) - \Gamma_\mu(n) U_{-\mu}(n) \psi(n - \hat{\mu}) \right), \quad (3.21)$$

and

$$S_f^\theta[x, \bar{\psi}, \psi, U] = \sum_{n \in \Lambda} V^\theta(n) \bar{\psi}(n) (D_{\text{naive}}^\theta \psi)(n). \quad (3.22)$$

Finally set

$$S_f[x, \bar{\psi}, \psi, U] = \frac{1}{2} \left( S_f^\circ[x, \bar{\psi}, \psi, U] + S_f^\theta[x, \bar{\psi}, \psi, U] \right). \quad (3.23)$$

On a regular embedding  $x(n) = a n$ , the forward and backward corner frames coincide (with our convention for  $E^\theta$ ), so  $\Gamma_\mu(n) = \Gamma_\mu^\theta(n) = \gamma_\mu/a$ , and (3.19) reduces to the usual naive lattice Dirac operator. As the standard lattice is among the possible embeddings  $x(n)$ , we do not expect the dynamical geometry alone to remove species doubling. Standard remedies (Wilson, staggered, overlap, domain-wall) can nevertheless be implemented by replacing the corresponding finite-difference operators and Wilson terms by their geometric analogues built from the same local data  $(E, g, V)$  and then applying the  $\theta$ -averaging prescription (3.6).

**Total field action.** In the sequel we write

$$S_{\text{fields}}[x, U, \Phi] := S_g[x, U] + S_\phi[x, \phi, U] + S_f[x, \bar{\psi}, \psi, U] + \dots, \quad (3.24)$$

where the ellipsis indicates additional matter multiplets treated analogously. By construction,  $S_{\text{fields}}$  is local on the abstract lattice, gauge invariant, and  $\Theta$ -invariant under the OS reflection introduced later.

### 3.2 Euclidean invariance, orientation, and local isotropy

We record the global Euclidean symmetries of the action and make explicit where a restriction to proper motions enters. Recall that the Euclidean group is the semidirect product

$$E(d) = O(d) \ltimes \mathbb{R}^d, \quad (3.25)$$

with multiplication  $(R, b)(R', b') = (RR', b + Rb')$ . We write  $SE(d) = SO(d) \ltimes \mathbb{R}^d$  for the subgroup of *proper* Euclidean motions.

Let  $(R, b) \in E(d)$  act on a configuration  $(x, U, \Phi)$  by

$$\begin{aligned} x(n) &\mapsto x'(n) := Rx(n) + b, \\ U_\mu(n) &\mapsto U'_\mu(n) := U_\mu(n), \\ \Phi(n) &\mapsto \Phi'(n) := \rho(R) \Phi(n), \end{aligned} \quad (3.26)$$

where  $\rho$  is the appropriate finite-dimensional representation of  $O(d)$  on the matter field (trivial for scalars; spinorial for Dirac fields, discussed below). Since  $b$  is a translation in physical space, it acts trivially on internal indices.

The edge vectors transform as

$$e_\mu(n) = x(n + \hat{\mu}) - x(n) \mapsto e'_\mu(n) = x'(n + \hat{\mu}) - x'(n) = R e_\mu(n), \quad (3.27)$$

hence the local frame matrix  $E(n) = [e_1(n) \cdots e_d(n)]$  transforms as  $E'(n) = RE(n)$ . Therefore the Gram matrix is strictly invariant:

$$g'(n) = E'(n)^\top E'(n) = E(n)^\top R^\top RE(n) = g(n). \quad (3.28)$$

For the local cell volume there are two closely related quantities:

$$\det E'(n) = (\det R) \det E(n), \quad |\det E'(n)| = |\det E(n)|, \quad (3.29)$$

so the *unoriented* volume  $V(n) = |\det E(n)|$  is invariant under all of  $O(d)$ , while the *oriented* volume  $\det E(n)$  is invariant only under  $SO(d)$ .

**Invariance of the geometry action.** Suppose the geometry action has the local form

$$S_x[x] = \sum_{n \in \Lambda} s_x(g(n), g(n)^{-1}, V(n)), \quad (3.30)$$

or more generally depends on  $x$  only through scalar functions of the Gram matrix (e.g. eigenvalues of  $g(n)$ ,  $\text{Tr } g(n)$ ,  $V(n)$ , etc.). Then (3.28) and  $V'(n) = V(n)$  imply

$$S_x[x'] = S_x[x] \quad \text{for all } (R, b) \in E(d). \quad (3.31)$$

If, instead, one chooses to build  $S_x$  from the *oriented* determinant  $\det E(n)$ , then  $S_x$  is automatically  $SE(d)$ -invariant, but is *not* invariant under reflections with  $\det R = -1$  unless  $s_x$  is an even function of  $\det E(n)$ .

**Orientation flipping.** The preceding statements concern the integrand (action) as a function of an *arbitrary* embedding. The subtlety is that our *configuration space* for  $x$  is typically restricted by a hard admissibility condition that fixes an orientation, e.g.

$$\det E(n) \geq V_{\min} > 0 \quad \text{for all } n. \quad (3.32)$$

This condition is stable under  $SE(d)$  but not under a reflection: if  $\det R = -1$  then  $\det E'(n) = -\det E(n) \leq -V_{\min}$ , so  $x' \notin \mathcal{X}_{\text{adm}}$  even though  $g'(n) = g(n)$  and  $|\det E'(n)| = |\det E(n)|$ . Thus:

*The local geometric quantities and the local action density can be  $E(d)$ -invariant, but the domain of integration  $\mathcal{X}_{\text{adm}}$  is typically only  $SE(d)$ -invariant when one imposes a positive-orientation constraint.*

Choice of orientation breaks *explicit* invariance under improper Euclidean motions (parity / reflections) at finite lattice spacing. This is a regulator-level choice of orientation sector, and we expect it to be innocuous for the continuum limit of parity-even observables. One could restore exact  $E(d)$  invariance by integrating over both orientation components, at the cost of enlarging configuration space. This orientation restriction does *not* interfere with Osterwalder–Schrader reflection positivity: the OS involution  $\Theta$  is constructed so that  $\Theta \mathcal{X}_{\text{adm}} = \mathcal{X}_{\text{adm}}$  (Lemma 4.1), even though  $\Theta$  contains a target-space reflection.

**Exact symmetry of the regulator.** The partition function is defined as

$$Z = \int_{\mathcal{X}_{\text{adm}}} Dx \int DU \int D\Phi \exp(-S_x[x] - S_{\text{fields}}[x, U, \Phi]). \quad (3.33)$$

Since the flat product measure  $Dx$  and the Haar/product measures  $DU$ ,  $D\Phi$  are invariant under (3.26), and since  $\mathcal{X}_{\text{adm}}$  is stable precisely under  $SE(d)$ , the regulator has an *exact* global  $SE(d)$  symmetry, provided the field action is  $SE(d)$ -invariant:

$Z$  and all expectation values of observables are invariant under  $(R, b) \in \text{SE}(d)$ .

If one wishes to be fully precise, the definition is made first on a finite region  $\Lambda_{T,L}$ , so that  $Dx, DU, D\Phi$  are ordinary finite product measures, and the  $\text{SE}(d)$  covariance holds there exactly; the infinite-volume partition function is then understood formally, while expectations of local observables are defined by the limit  $\Lambda_{T,L} \nearrow \mathbb{Z}^d$ .

To verify global Euclidean invariance for the field action, it suffices to only deal with the prototype part  $S^\circ$ . Indeed, under  $x(n) \mapsto Rx(n) + b$ , the advanced and retarded frames transform as  $E(n) \mapsto RE(n)$  and  $E^\theta(n) \mapsto RE^\theta(n)$ , so any coefficient built from Euclidean invariants is unchanged; the relabeling  $\mu \mapsto \theta(\mu)$  is purely combinatorial. Therefore  $S^\theta$  inherits the same  $\text{SE}(d)$ -invariance as  $S^\circ$ , and so does the averaged action  $\frac{1}{2}(S^\circ + S^\theta)$ .

**Scalar actions.** Consider the gauge-covariant forward difference (3.7). Under (3.26), we have  $|e'_\mu(n)| = |Re_\mu(n)| = |e_\mu(n)|$ ,  $U'_\mu = U_\mu$ , and  $\phi'(n) = \rho(R)\phi(n)$ , hence

$$\nabla_\mu \phi'(n) = \rho(R) \nabla_\mu \phi(n). \quad (3.34)$$

Assuming the internal inner product on the scalar multiplet is  $O(d)$ -invariant (as in the usual continuum theory), we obtain pointwise invariance of the kinetic density:

$$\sum_{\mu, \nu=1}^d g^{\mu\nu}(n) \langle \nabla_\mu \phi'(n), \nabla_\nu \phi'(n) \rangle = \sum_{\mu, \nu=1}^d g^{\mu\nu}(n) \langle \nabla_\mu \phi(n), \nabla_\nu \phi(n) \rangle, \quad (3.35)$$

since  $g^{\mu\nu}(n)$  is invariant and  $\rho(R)$  preserves the inner product. Multiplying by  $V(n) = |\det E(n)|$  and summing over  $n$  yields

$$S_{\phi, \text{kin}}^\circ[x', \phi', U'] = S_{\phi, \text{kin}}^\circ[x, \phi, U]. \quad (3.36)$$

The potential term  $S_{\phi, \text{pot}}^\circ = \sum_n V(n) W_{\text{loc}}(\phi(n))$  is also invariant provided  $W_{\text{loc}}$  is an  $O(d)$ -scalar in field space (e.g.  $\frac{1}{2}m_0^2|\phi|^2 + \frac{1}{4!}\lambda_0|\phi|^4$ ).

**Gauge actions.** For the weighted Wilson-type plaquette action (3.14) the gauge field  $U$  is unchanged by  $(R, b) \in \text{E}(d)$ , so the traces are invariant. Therefore  $S_g$  is  $E(d)$ -invariant provided each weight  $w^{\mu\nu}(n; x)$  is built from Euclidean invariants of the local geometry (equivalently, from  $g_{\mu\nu}(n)$ ,  $g^{\mu\nu}(n)$ ,  $V(n)$ , and Gram minors). In particular this holds for both weight choices introduced in (3.15) and (3.16). Note that as in the continuum, weights built from oriented pseudoscalars would be sensitive to improper rotations.

**Fermionic actions.** In the presence of Dirac fields we work with the proper Euclidean group  $\text{SE}(d) = \text{SO}(d) \times \mathbb{R}^d$ , since implementing reflections on spinors would require the Pin group. Independently, our admissible set  $\mathcal{X}_{\text{adm}}$  fixes an orientation component, so the  $x$ -measure is restricted to  $\text{SE}(d)$  rather than  $\text{E}(d)$ .

Let  $R \in \text{SO}(d)$  and choose a lift  $\hat{R} \in \text{Spin}(d)$  acting on spinors by  $\psi'(n) = \hat{R}\psi(n)$  and  $\bar{\psi}'(n) = \bar{\psi}(n)\hat{R}^{-1}$ , with the standard intertwining property

$$\hat{R}\gamma_a\hat{R}^{-1} = R_a{}^b\gamma_b. \quad (3.37)$$

Under  $x'(n) = Rx(n) + b$  the local frame matrices transform by  $E'(n) = RE(n)$  and likewise  $E^{\theta'}(n) = RE^\theta(n)$ , since both are built from the same local edge vectors of the embedding. Consequently the geometry-dependent matrices  $\Gamma_\mu(n)$  and  $\Gamma_\mu^\theta(n)$  transform by conjugation:

$$\hat{R}\Gamma_\mu(n)\hat{R}^{-1} = \sum_a \hat{R}\gamma_a\hat{R}^{-1}(E^{-1})_{a\mu} = \sum_{a,b} R_a{}^b\gamma_b(E^{-1})_{a\mu} = \sum_b \gamma_b(E'^{-1})_{b\mu} = \Gamma'_\mu(n), \quad (3.38)$$

and similarly  $\widehat{R}\Gamma_\mu^\theta(n)\widehat{R}^{-1} = \Gamma_\mu^{\theta'}(n)$ . Since the gauge links  $U_\mu(n)$  are unchanged by Euclidean motions and act only on gauge indices, the mixed prototype naive Dirac operator (3.19) transforms covariantly:

$$(D_{\text{naive}}^\circ\psi')(n) = \widehat{R}(D_{\text{naive}}^\circ\psi)(n). \quad (3.39)$$

Using also  $V'(n) = V(n)$  (and  $V^{\theta'}(n) = V^\theta(n)$ ) we conclude invariance of the prototype action:

$$S_f^\circ[x', \bar{\psi}', \psi', U] = \sum_n V(n) \bar{\psi}(n) \widehat{R}^{-1} \widehat{R} (D_{\text{naive}}^\circ\psi)(n) = S_f^\circ[x, \bar{\psi}, \psi, U]. \quad (3.40)$$

**Local isotropy via twisting.** It is useful to separate two notions that are sometimes conflated under the phrase “rotationally invariant regulator.” The first is the *exact* global covariance of the partition function under  $\text{SE}(d)$ , which follows formally because the action depends on the embedding only through Euclidean invariants. However, this formal covariance is not, by itself, the operative mechanism at finite cutoff: it would remain true even if the geometry measure were concentrated near a rigid  $\text{SE}(d)$ -orbit  $x(n) \approx aRn + b$ , in which case typical configurations exhibit essentially no local orientation mixing and one recovers the usual hypercubic anisotropies. What matters is therefore *how* global  $\text{SE}(d)$  covariance is realised in typical configurations after fixing/quotienting the global zero modes.

The second notion is a *local isotropy* (or local orientation–mixing) property. In the short-range geometry regime (SR) required for a local Symanzik description after integrating out geometry, the geometry sector cannot realise  $\text{SE}(d)$  covariance “rigidly” through long-range geometric modes; rather, global covariance must be implemented through *short-range fluctuations of local frames*. We make this precise by extracting from the embedding a local orientation field. Define the dimensionless forward frame  $\tilde{E}(n) = a^{-1}E(n)$ . By admissibility  $\tilde{E}(n)$  is invertible, hence it has a polar decomposition

$$\tilde{E}(n) = Q(n)S(n), \quad Q(n) \in \text{SO}(d), \quad S(n) \in \text{SPD}(d). \quad (3.41)$$

Note that  $\det \tilde{E}(n) > 0$  by admissibility, so the polar factor  $Q(n)$  lies in  $\text{SO}(d)$ . We interpret  $Q(n)$  as the *local orientation* and  $S(n)$  as the *local shape*.

From  $Q(n)$  we build an  $\text{SO}(d)$ -valued discrete connection on links,

$$R_\mu(n) = Q(n)^{-1}Q(n + \hat{\mu}) \in \text{SO}(d), \quad (3.42)$$

and a plaquette holonomy (curvature proxy)

$$\mathcal{R}_{\mu\nu}(n) = R_\mu(n)R_\nu(n + \hat{\mu})R_\mu(n + \hat{\nu})^{-1}R_\nu(n)^{-1} \in \text{SO}(d). \quad (3.43)$$

These observables distinguish rigid orbit averaging from genuine local twisting: if  $x(n) = aRn + b$  is rigid then  $Q(n) \equiv R$  and hence  $R_\mu(n) \equiv I$  and  $\mathcal{R}_{\mu\nu}(n) \equiv I$ ; conversely, broad fluctuations of  $R_\mu$  together with short-range decorrelation indicate nontrivial local twisting.

*Local isotropy is a statistical property, not an exact local symmetry.* There is no underlying local  $\text{SO}(d)$  gauge redundancy; rather, the mechanism is that the distribution of  $R_\mu(n)$  is sufficiently mixing and its correlations decay rapidly. We could quantify this via class functions  $f : \text{SO}(d) \rightarrow \mathbb{R}$  (e.g.  $f(R) = \text{tr}(R)$ ) and the connected correlator

$$\langle f(R_\mu(n)) f(R_\mu(m)) \rangle_c, \quad (3.44)$$

where  $\langle AB \rangle_c = \langle AB \rangle - \langle A \rangle \langle B \rangle$  denotes the connected correlator. The quantity (3.44) measures how rapidly the local frame rotations decorrelate with separation. In a near-rigid regime (dominated by

global zero modes) one has  $R_\mu(n) \approx I$  and the fluctuations of  $R_\mu$  are small and long-range, whereas in a genuine twisting regime the distribution of  $R_\mu(n)$  is broad and the connected correlator decays on a short correlation length  $\xi_{\text{twist}}$  (typically a few lattice spacings). This short-range mixing of local orientations is precisely the ingredient that can reduce axis-versus-diagonal (direction-dependent) cutoff artefacts in matter correlators at finite  $a$ .

### 3.3 Gauge invariance and lattice symmetries

We briefly recall the gauge and lattice symmetries of the dynamical–lattice regulator. These act on the abstract hypercubic graph  $\Lambda$  and on the gauge/matter fields, while the geometry field  $x$  is gauge neutral and transforms only under global Euclidean transformations (§3.2).

**Gauge invariance.** Let  $G$  be a compact gauge group and let

$$\Omega : \Lambda \rightarrow G, \quad n \mapsto \Omega(n), \quad (3.45)$$

be a lattice gauge transformation. We let  $\Omega$  act on the link variables and on the matter fields in the usual way:

$$U_\mu(n) \mapsto U_\mu^\Omega(n) := \Omega(n)U_\mu(n)\Omega(n + \hat{\mu})^{-1}, \quad (3.46)$$

$$\Phi(n) \mapsto \Phi^\Omega(n) := \rho_m(\Omega(n))\Phi(n), \quad (3.47)$$

where  $\rho_m$  is the representation of  $G$  carried by the matter multiplet. The geometry field  $x(n)$  is unaffected:

$$x(n) \mapsto x^\Omega(n) := x(n). \quad (3.48)$$

As in the Euclidean invariance case, gauge invariance need only be verified for the prototype action  $S^\circ$ , since  $S^\theta$  is defined by the same local stencils with direction labels relabeled by  $\mu \mapsto \theta(\mu)$  and with geometry-dependent weights replaced by functions of  $x$  only. As these operations commute with the local gauge transformation (3.46)–(3.47), we have  $S^\theta[U^\Omega, \Phi^\Omega] = S^\theta[U, \Phi]$ , and hence the averaged action is gauge invariant.

By construction the prototype action  $S_{\text{fields}}^\circ[x, U, \Phi]$  is a sum of gauge invariant local terms built from traces of Wilson loops and gauge covariant combinations of  $\Phi$  and its lattice covariant derivatives. For example, the gauge part of the action may be written as

$$S_g^\circ[x, U] = \sum_{n, \mu < \nu} w^{\mu\nu}(x; n) \Re \text{tr}(I - U_{\mu\nu}(n)), \quad (3.49)$$

with local geometry–dependent weights  $w_{\mu\nu}(x; n)$  and plaquette variables  $U_{\mu\nu}(n)$  built from the links  $U_\mu(n)$  in the usual way. Under (3.46) the plaquettes transform by conjugation and the traces are invariant. Likewise, the matter part of  $S_{\text{fields}}^\circ$  is built from gauge covariant bilinears such as  $\bar{\Phi}(n)\Phi(n)$  and  $\bar{\Phi}(n)D_\mu\Phi(n)$ , which are invariant under (3.47). Since  $x$  is gauge neutral and appears only through gauge invariant weights such as  $w_{\mu\nu}(x; n)$ , we have

$$S_{\text{fields}}^\circ[x, U^\Omega, \Phi^\Omega] = S_{\text{fields}}^\circ[x, U, \Phi] \quad \text{for all } \Omega : \Lambda \rightarrow G, \quad (3.50)$$

so the full action (3.1) is gauge invariant for every geometry configuration  $x \in \mathcal{X}_{\text{adm}}$ . The geometry action  $S_x[x]$  is gauge invariant trivially, as it depends only on  $x$ .

**Lattice translations and hypercubic symmetries.** In addition to gauge transformations, the theory is invariant under lattice translations and under those hypercubic relabellings of the

abstract lattice that preserve the admissible domain  $\mathcal{X}_{\text{adm}}(a)$ . Let  $\tau_k : \Lambda \rightarrow \Lambda$  be the translation  $\tau_k(n) = n + k$ , and let

$$\mathbf{H}(d) = \{R \in \text{GL}(d, \mathbb{Z}) : R^T R = I\}, \quad \mathbf{H}^+(d) = \{R \in \mathbf{H}(d) : \det R = +1\}. \quad (3.51)$$

We let these maps act on fields by pullback:

$$(\tau_k x)(n) := x(n - k), \quad (\tau_k \Phi)(n) := \Phi(n - k), \quad (\tau_k U)(\ell) := U(\tau_k^{-1} \ell), \quad (3.49)$$

and for  $R_{\text{lat}} \in \mathbf{H}(d)$ ,

$$(R_{\text{lat}} x)(n) := x(R_{\text{lat}}^{-1} n), \quad (R_{\text{lat}} \Phi)(n) := \Phi(R_{\text{lat}}^{-1} n), \quad (R_{\text{lat}} U)(\ell) := U(R_{\text{lat}}^{-1} \ell), \quad (3.50)$$

where  $U$  is viewed as a function on oriented links  $\ell = (n \rightarrow n + \hat{\mu})$ , and  $R_{\text{lat}}$  acts on oriented links in the obvious way. Since the action is a sum of identical local stencil terms and the product measures are invariant under relabelling of factors (including  $U \mapsto U^{-1}$  on links by Haar invariance), these transformations preserve the action and measure whenever they preserve  $\mathcal{X}_{\text{adm}}(a)$ .

With the basic definition of  $\mathcal{X}_{\text{adm}}(a)$  in terms of a distinguished corner frame and a selected orientation component, we therefore only claim invariance under the corresponding subgroup of  $\mathbf{H}^+(d)$  that fixes that corner choice. If instead one imposes the strengthened all-corner oriented-volume condition of Remark 2.4(A3), then  $\mathcal{X}_{\text{adm}}(a)$  is invariant under the full orientation-preserving hypercubic group  $\mathbf{H}^+(d)$ . Permutations with  $\det = -1$  exchange the two orientation components and hence would not be included.

**Locality.** We say that a functional  $F[x, U, \Phi]$  is *local* if it can be written as a sum of terms

$$F[x, U, \Phi] = \sum_{n \in \Lambda} f_n, \quad (3.52)$$

where each  $f_n$  depends only on the restriction of  $(x, U, \Phi)$  to a finite neighbourhood of  $n$ , with a radius (in lattice distance) that is independent of  $n$  and of the lattice size. In particular, the geometry action  $S_x[x]$  in (2.20) and the field action  $S_{\text{fields}}[x, U, \Phi]$  are local in this sense: the local density at site  $n$  depends on the geometry only through the frame  $E(n)$ , or a bounded stencil of neighbouring frames, and on the gauge/matter fields only through fields on a fixed finite stencil of sites and links around  $n$ .

Thus, at the level of the abstract graph, the dynamical-lattice regulator has exactly the same locality and lattice symmetry structure as standard hypercubic lattice gauge theory. The only difference is that the local couplings are promoted to functions of the dynamical geometry via the metric  $g(n)$  and volume  $V(n)$ . The global Euclidean invariance in the embedding space  $\mathbb{R}^d$  is an additional continuous symmetry acting on  $x$ , which we discussed in Section 3.2.

### 3.4 Viewpoint as an extended lattice field theory

It is conceptually useful to reinterpret the dynamical-lattice regulator purely as a lattice field theory on the abstract hypercubic graph  $\Lambda$ , with an enlarged field content. Instead of thinking of  $x : \Lambda \rightarrow \mathbb{R}^d$  as an embedding, one may regard its Cartesian components  $x_\mu(n)$  as additional real scalar fields attached to sites or links. From this point of view the configuration space is simply

$$\{x_\mu(n), U_\mu(n), \Phi(n) : n \in \Lambda, \mu = 1, \dots, d\}, \quad (3.53)$$



and the geometry–dependent quantities  $e_\mu(n)$ ,  $g_{\mu\nu}(n)$  and  $V(n)$  are just local composite fields built from the  $x_\mu(n)$  on a finite stencil. The action  $S[x, U, \Phi]$  defined in (3.1) is then a sum of strictly local terms on this extended field space, and the path integral (3.2) is an ordinary Euclidean lattice path integral with local interactions.

In this extended viewpoint the main structural properties of the regulator follow from standard lattice arguments applied to the enlarged field content. Locality and gauge invariance are manifest at the level of the abstract graph, as discussed in Section 3.3. Reflection positivity is proved by choosing a reflection of the time index  $n_1$  on  $\Lambda$  and checking the usual Osterwalder–Schrader inequalities for the extended field multiplet  $(x, U, \Phi)$ ; the detailed construction of the reflection, the splitting of the lattice into time slices, and the verification of the OS axioms are carried out in Section 4. In particular, no continuum notion of “time” or preferred coordinate direction in  $\mathbb{R}^d$  is required at the microscopic level: all reflection operations are defined purely on the index lattice, and the embedding variables  $x_\mu(n)$  enter only through local, reflection invariant combinations. This perspective makes clear that the dynamical–lattice regulator fits squarely within the usual constructive framework for Euclidean lattice field theory, with the dynamical geometry fields providing an  $E(d)$ –invariant way of dressing local couplings without sacrificing locality or reflection positivity.

## 4 Reflection positivity and continuum universality

In this section we first establish Osterwalder–Schrader (OS) reflection positivity for a large class of DLR, and briefly recall the associated Hilbert space reconstruction. We then discuss the Symanzik effective action description of the continuum limit and explain why, under mild assumptions on the geometry sector, the dynamical–lattice theory lies in the same universality class as the corresponding theory on a static hypercubic lattice. As a concrete check we sketch the one–loop running of the quartic coupling in scalar  $\phi^4$  theory.

### 4.1 Reflection positivity for the bosonic sector

In this subsection we treat the bosonic matter sector, i.e., gauge fields coupled to complex scalar fields  $\phi$ ; the fermionic sector is treated separately in the next subsection.

Note that for a *generic* admissible embedding  $x \in \mathcal{X}_{\text{adm}}$ , the induced matter/gauge action need not be reflection symmetric *at fixed*  $x$ . Accordingly, we cannot hope to obtain “conditional” OS positivity at fixed geometry. Instead, we establish reflection positivity directly for the *joint* Euclidean measure of the extended field multiplet  $\omega = (x, U, \phi)$ .

We single out the first lattice direction  $n_1$  as Euclidean time and use the *link reflection*

$$\theta(n_1, n_2, \dots, n_d) = (1 - n_1, n_2, \dots, n_d). \quad (4.1)$$

This induces the reflection  $\theta\mu$  on directions  $\mu$  as in (3.4), and the OS involution  $\Theta$  on  $\omega$  by

$$(\Theta x)(n) = r(x(\theta n)), \quad (\Theta U)_\mu(n) = U_{\theta\mu}(\theta n), \quad (\Theta \phi)(n) = \overline{\phi(\theta n)}, \quad (4.2)$$

where  $r \in O(d)$  is the target space reflection  $r(v_1, v_2, \dots, v_d) = (-v_1, v_2, \dots, v_d)$ , the reflection  $\theta\mu$  on the direction  $\mu$  is as in (3.4), and the overline denotes complex conjugation.

**Lemma 4.1.** We have  $x \in \mathcal{X}_{\text{adm}}(a)$  if and only if  $\Theta x \in \mathcal{X}_{\text{adm}}(a)$ .

*Proof.* Let us encode the dependence of  $e_\mu$  on the embedding  $x$  as

$$e_\mu(x; n) = x(n + \hat{\mu}) - x(n), \quad \mu \in \Delta. \quad (4.3)$$

Then (4.2) gives

$$\begin{aligned} e_\mu(\Theta x; n) &= (\Theta x)(n + \hat{\mu}) - (\Theta x)(n) = rx(\theta(n + \hat{\mu})) - rx(\theta n) \\ &= r(x(\theta n + \widehat{\theta\mu}) - x(\theta n)) = r e_{\theta\mu}(x; \theta n). \end{aligned} \quad (4.4)$$

Since  $r \in O(d)$ , we have  $|e_\mu(\Theta x; n)| = |e_{\theta\mu}(x; \theta n)|$ . Therefore any uniform length bounds imposed on  $\{|e_\mu(n)| : \mu \in \Delta\}$  are preserved, up to the harmless relabelling  $n \mapsto \theta n$ .

Applying (4.4) to  $E$  and  $E^\theta$  columnwise gives

$$E(\Theta x; n) = rE^\theta(x; \theta n), \quad E^\theta(\Theta x; n) = rE(x; \theta n). \quad (4.5)$$

Taking determinants and using  $\det(r) = -1$  yields

$$\det E(\Theta x; n) = -\det E^\theta(x; \theta n), \quad \det E^\theta(\Theta x; n) = -\det E(x; \theta n), \quad (4.6)$$

so the oriented volume bounds appearing in Definition 2.1 are mapped into each other, again up to relabelling  $n \mapsto \theta n$ . Hence  $\Theta$  maps  $\hat{\mathcal{X}}_{\text{adm}}(a)$  bijectively to itself.

Finally,  $\Theta$  is continuous and  $\Theta^2 = \text{id}$ , so it maps connected components of  $\hat{\mathcal{X}}_{\text{adm}}(a)$  to connected components. Since  $\Theta x_{\text{reg}} = x_{\text{reg}}$ , the principal component containing  $x_{\text{reg}}$  is preserved. Therefore  $\Theta(\mathcal{X}_{\text{adm}}(a)) = \mathcal{X}_{\text{adm}}(a)$ , which proves the claim.  $\square$

We consider the probability measure

$$d\mu(\omega) = \frac{1}{Z} \mathbf{1}_{\{x \in \mathcal{X}_{\text{adm}}\}} \exp(-S_x[x] - S_{\text{fields}}[x, U, \phi]) Dx DU D\phi, \quad (4.7)$$

where  $Dx$  is the product Lebesgue measure on  $(\mathbb{R}^d)^\Lambda$ , and  $DU, D\phi$  are the usual Haar/Lebesgue measures for the gauge/matter fields. We first note that Lemma 4.1 implies that the hard constraint  $\mathbf{1}_{\{x \in \mathcal{X}_{\text{adm}}(a)\}}$  is invariant under  $\Theta$ . Moreover, the geometric and field actions will always be taken to be local and  $\Theta$ -invariant. For the concrete examples of Section 3.1 this invariance holds by design, and in general it is a standing assumption on the choice of  $S_x$  and  $S_{\text{fields}}$ . Thus, to establish  $\Theta$ -invariance of (4.7) it remains to check  $\Theta$ -invariance of the product measures  $Dx, DU$  and  $D\phi$ .

To make these statements completely precise one should work at finite volume, where all measures are honest finite products. We therefore fix a finite cylinder

$$\Lambda_{T,L} = \{1 - T, \dots, 0, 1, \dots, T\} \times (\mathbb{Z}/L\mathbb{Z})^{d-1}, \quad (4.8)$$

with open boundary conditions in the time direction and periodic boundary conditions in space. All local action terms are defined by the same formulas as on  $\mathbb{Z}^d$ , but we include a term in the finite-volume sum only if every site/link variable appearing in its stencil lies in  $\Lambda_{T,L}$ . Equivalently, for each local contribution  $t_n(\varepsilon)$  anchored at a basepoint  $n$ , we keep  $t_n$  iff  $\text{stencil}(t_n) \subset \Lambda_{T,L}$ ; otherwise it is omitted. For nearest-neighbour actions this removes only the finitely many terms that would require sites outside the time boundaries.

All local action terms are defined by the same formulas as on  $\mathbb{Z}^d$ , and we sum only over those basepoints for which every site/link appearing in the corresponding finite stencil lies in  $\Lambda_{T,L}$ . In

particular, for the two-frame geometry data  $(E, E^\theta)$  we only use sites  $n$  for which both  $n \pm \hat{1} \in \Lambda_{T,L}$  (spatial neighbours exist by periodicity).

We define the finite-volume admissible set  $\mathcal{X}_{\text{adm}}^{T,L}(a)$  by imposing the  $a$ -admissibility inequalities only at those sites  $n \in \Lambda_{T,L}$  for which the required neighbour stencil is contained in  $\Lambda_{T,L}$ . With this convention the index set of admissibility constraints is  $\theta$ -invariant, hence so is  $\mathcal{X}_{\text{adm}}^{T,L}(a)$ . For notational simplicity we will not introduce a special notation for finite-volume objects: in what follows  $\Lambda$ ,  $Dx$ ,  $DU$ ,  $D\phi$ , and  $\mathcal{X}_{\text{adm}}(a)$  refer to the above finite cylinder, and all identities are proved at fixed  $(T, L)$  and then interpreted on the infinite lattice by taking  $T, L \rightarrow \infty$  on local observables.

**Lemma 4.2.** The product measures  $Dx$ ,  $DU$  and  $D\phi$  are invariant under  $\Theta$ .

*Proof.* At finite volume all measures are honest finite products, so it suffices to check invariance factor by factor. The map  $x \mapsto \Theta x$  is given by  $(\Theta x)(n) = r(x(\theta n))$ : it permutes the site labels and applies the same orthogonal map  $r \in O(d)$  to each  $x(n) \in \mathbb{R}^d$ . A permutation of factors preserves a product Lebesgue measure, and an orthogonal map has  $|\det r| = 1$ , hence  $Dx = \prod_n d^d x(n)$  is  $\Theta$ -invariant.

For a complex scalar multiplet,  $(\Theta\phi)(n) = \overline{\phi(\theta n)}$  is again a site permutation composed with complex conjugation, which is an orthogonal linear map on  $\mathbb{R}^{2m}$  and therefore preserves Lebesgue measure; thus  $D\phi$  is  $\Theta$ -invariant. Obviously, for real multiplets the conjugation is absent.

Finally, view the gauge field as assigning a group element to each oriented link. Under link reflection,  $\Theta$  maps each link variable to another link variable or to its inverse. Since Haar measure on a compact Lie group is invariant under inversion  $U \mapsto U^{-1}$  and under relabelling of factors, the product Haar measure  $DU$  is  $\Theta$ -invariant.  $\square$

We state the reflection-positivity criterion for the coupled DLR measure. In the concrete examples of §3.1, the total action  $S = S_x + S_{\text{fields}}$  is local on the abstract lattice and is  $\Theta$ -invariant by construction (each prototype term is paired with its  $\theta$ -partner and then averaged), and the admissible set  $\mathcal{X}_{\text{adm}}(a)$  is  $\Theta$ -stable. In the theorem we abstract these features and assume only locality,  $\Theta$ -invariance, and finite interaction range in the index-time direction.

To define the positive-time algebra we fix the link reflection plane between the time slices  $n_1 = 0$  and  $n_1 = 1$  and write  $\Lambda = \Lambda_- \cup \Lambda_+$  with

$$\Lambda_- = \{n \in \Lambda : n_1 \leq 0\}, \quad \Lambda_+ = \{n \in \Lambda : n_1 \geq 1\}. \quad (4.9)$$

We say that a functional  $F(\omega)$  is *supported in*  $\Lambda_+$  if it depends only on (i) site variables located at sites  $n \in \Lambda_+$ , and (ii) link variables  $U_\mu(n)$  whose two endpoints  $n$  and  $n + \hat{\mu}$  both lie in  $\Lambda_+$ . In particular, the support convention forbids dependence on any link variable whose endpoints lie on opposite sides of the reflection plane.

Let  $\mathcal{A}_+$  be the algebra generated by bounded functionals supported in  $\Lambda_+$ , and define  $\Theta F$  by

$$(\Theta F)(\omega) = \overline{F(\Theta\omega)}, \quad \omega = (x, U, \phi), \quad (4.10)$$

where the overline denotes complex conjugation. In particular,  $\Theta$  is antilinear. With the above support convention,  $\Theta$  maps  $\mathcal{A}_+$  into the corresponding algebra on  $\Lambda_-$ .

Here and below, for functionals  $F, G$  on configuration space we write  $(F \cdot G)(\omega) = F(\omega) G(\omega)$  for their pointwise product, so that  $\langle \Theta F \cdot F \rangle = \int (\Theta F)(\omega) F(\omega) d\mu(\omega)$ .

**Theorem 4.3.** Assume that the total action  $S = S_x + S_{\text{fields}}$  is local and  $\Theta$ -invariant, i.e.

$$S[\Theta x, \Theta U, \Theta \phi] = S[x, U, \phi] \quad \text{for all } x \in \mathcal{X}_{\text{adm}}(a), \quad (4.11)$$

and that the interaction has finite range in the index–time direction: there exists an integer  $\ell \geq 1$  such that each local term in  $S$  depends only on variables whose site time–indices  $n_1$  lie in an interval of length at most  $\ell$  (equivalently, the  $n_1$ –diameter of the stencil is  $\leq \ell$ ). Then

$$\langle \Theta F \cdot F \rangle \geq 0 \quad \text{for all } F \in \mathcal{A}_+, \quad (4.12)$$

where  $\langle \cdot \rangle$  denotes expectation with respect to the joint measure (4.7).

*Proof.* We use the standard link–reflection factorization argument. Fix  $\ell$  as in the hypothesis and introduce the finite reflection slab

$$\Sigma_\ell = \{n \in \Lambda : 1 - \ell \leq n_1 \leq \ell\}.$$

For the nearest–neighbour/plaquette actions of §3.1 one has  $\ell = 1$ , hence  $\Sigma_\ell = \{n_1 \in \{0, 1\}\}$ . Decompose a configuration as  $\omega = (\omega_-, \omega_0, \omega_+)$  by declaring: (i)  $\omega_0$  consists of all site variables  $(x(n), \phi(n))$  with  $n \in \Sigma_\ell$ , together with all link variables  $U_\mu(n)$  whose link  $\{n, n + \hat{\mu}\}$  meets  $\Sigma_\ell$ ; (ii)  $\omega_+$  consists of the remaining variables with support in the strict future  $\{n_1 \geq \ell + 1\}$  (sites) and links with both endpoints in  $\{n_1 \geq \ell + 1\}$ ; and (iii)  $\omega_-$  consists of the remaining variables with support in the strict past  $\{n_1 \leq -\ell\}$  (sites) and links with both endpoints in  $\{n_1 \leq -\ell\}$ .

By the finite time–range assumption, no local interaction term can simultaneously involve variables from the strict past  $\{n_1 \leq -\ell\}$  and the strict future  $\{n_1 \geq \ell + 1\}$ . Hence every local term belongs to exactly one of the following three classes: it is supported entirely in  $\Sigma_\ell$ ; or it involves at least one variable from the strict future; or it involves at least one variable from the strict past. Therefore the total action decomposes as

$$S(\omega) = S_+(\omega_0, \omega_+) + S_0(\omega_0) + S_-(\omega_0, \omega_-), \quad (4.13)$$

where  $S_0$  is the sum of all terms supported in  $\Sigma_\ell$ , and  $S_+$  (resp.  $S_-$ ) collects all remaining terms that involve at least one strict-future (resp. strict-past) variable; in particular  $S_+$  depends only on  $(\omega_0, \omega_+)$  and  $S_-$  only on  $(\omega_0, \omega_-)$ . Using that  $\mathcal{X}_{\text{adm}}$  is  $\Theta$ –stable and that the product measures are invariant under the induced relabelings, together with  $(\Theta F)(\omega) = \overline{F(\Theta\omega)}$ , one obtains

$$S_-(\omega_0, \omega_-) = (\Theta S_+)(\omega_0, \omega_-). \quad (4.14)$$

Now let  $F \in \mathcal{A}_+$ , so  $F$  depends only on the variables in  $\Lambda_+$  and thus only on  $(\omega_0, \omega_+)$ . Define

$$\Psi_F(\omega_0) = \int \exp(-S_+(\omega_0, \omega_+)) F(\omega_0, \omega_+) d\omega_+, \quad (4.15)$$

where  $d\omega_+$  denotes the product measure over the variables comprising  $\omega_+$ . Using  $\Theta$ –invariance of the domain and product measures together with (4.13)–(4.14) and  $(\Theta F)(\omega) = \overline{F(\Theta\omega)}$ , we obtain

$$\langle \Theta F \cdot F \rangle = \frac{1}{Z} \int \exp(-S_0(\omega_0)) \overline{\Psi_F(\omega_0)} \Psi_F(\omega_0) d\omega_0 = \frac{1}{Z} \int e^{-S_0(\omega_0)} |\Psi_F(\omega_0)|^2 d\omega_0 \geq 0, \quad (4.16)$$

which is (4.12). □

**Remark 4.4.** Only one reflection plane is needed for OS reconstruction. Site and link reflections, when both are available, differ by a one–step lattice translation. Here we work with the link reflection between the slices  $n_1 = 0$  and  $n_1 = 1$ .

## 4.2 Fermions and reflection positivity

We extend the coupled DLR measure to include fermions by introducing Grassmann-valued lattice spinors. Work at finite volume on the cylinder  $\Lambda = \Lambda_{T,L}$  as in the preceding subsection, with the understanding that statements on the infinite lattice are interpreted by taking the limit  $T, L \rightarrow \infty$  on local observables. At each site  $n \in \Lambda$  let  $\psi(n)$  and  $\bar{\psi}(n)$  be independent Grassmann generators, carrying spin and internal indices and transforming in a unitary representation of  $G$ . The fermionic integration is the Berezin product measure

$$D\bar{\psi} D\psi = \prod_{n \in \Lambda} \prod_{\alpha} d\bar{\psi}_{\alpha}(n) d\psi_{\alpha}(n),$$

for some fixed ordering of the site/index pairs.

We keep the support convention of the preceding subsection: a functional is supported in  $\Lambda_+$  if it depends only on site variables at sites  $n \in \Lambda_+$  and on link variables  $U_{\mu}(n)$  whose endpoints  $n$  and  $n + \hat{\mu}$  both lie in  $\Lambda_+$ . Let  $\mathcal{A}_+$  be the algebra generated by bounded bosonic functionals supported in  $\Lambda_+$  together with polynomials in the Grassmann generators  $\{\psi(n), \bar{\psi}(n)\}_{n \in \Lambda_+}$ . Let  $\mathcal{A}_+^{\text{even}} \subset \mathcal{A}_+$  denote its even subalgebra.

Fix constant Euclidean gamma matrices  $\{\gamma_a\}_{a=1}^d$  with  $\{\gamma_a, \gamma_b\} = 2\delta_{ab}$ . As in the standard lattice reflection-positivity setup, we take a representation in which the relevant transpose identities hold; concretely, it suffices that the gamma matrices are chosen so that the matrix involutions introduced below satisfy  $\Xi(n)^{\top} = \Xi(n)$  and  $\Xi(n)^2 = I$ .

Recall that the local frame matrix  $E(n)$  is built from the outgoing edge vectors at  $n$  and that  $E^{\theta}(n)$  denotes the time-reflected corner frame (same spatial columns, but using the backward time edge). From a frame  $E^{\sharp}(n)$ , which may be either  $E$  or  $E^{\theta}$ , we form the corresponding geometry-dependent Dirac matrices

$$\Gamma_{\mu}^{\sharp}(n) = \sum_{a=1}^d \gamma_a (E^{\sharp}(n)^{-1})_{a\mu}, \quad \{\Gamma_{\mu}^{\sharp}(n), \Gamma_{\nu}^{\sharp}(n)\} = 2g_{\sharp}^{\mu\nu}(n),$$

so in particular  $(\Gamma_1^{\sharp}(n))^2 = g_{\sharp}^{11}(n)I$  and the normalized matrix  $\hat{\Gamma}_1^{\sharp}(n) = \Gamma_1^{\sharp}(n)/\sqrt{g_{\sharp}^{11}(n)}$  is an involution,  $(\hat{\Gamma}_1^{\sharp}(n))^2 = I$ .

For the Osterwalder–Schrader reflection across the plane between  $n_1 = 0$  and  $n_1 = 1$  it is convenient to use, at each site, the normalized “time” matrix pointing *toward* the reflection plane:

$$\Xi(n) = \begin{cases} \hat{\Gamma}_1(n), & n \in \Lambda_- \text{ with } n_1 \leq 0, \\ \hat{\Gamma}_1^{\theta}(n), & n \in \Lambda_+ \text{ with } n_1 \geq 1. \end{cases} \quad (4.17)$$

This choice is entirely local (it uses only the corner frame attached to the site  $n$ ) and is tailored so that the same geometric “time direction toward the plane” is used on both sides. Other local choices of  $\Xi$  are possible; (4.17) is a particularly transparent one because it is an involution by construction and reduces to the constant matrix  $\gamma_1$  on a regular embedding.

Now define  $\Theta$  on the fermionic generators by

$$(\Theta\psi)(n) := \Xi(n) \bar{\psi}(\theta n)^{\top}, \quad (\Theta\bar{\psi})(n) := \psi(\theta n)^{\top} \Xi(n), \quad (4.18)$$

where  $^{\top}$  denotes transpose in the spin/internal indices (no complex conjugation is applied to the Grassmann generators themselves). On products and complex scalars we impose the graded anti-automorphism rules

$$\Theta(AB) = \Theta(B)\Theta(A), \quad \Theta(cA) = \bar{c}\Theta(A) \quad (c \in \mathbb{C}), \quad (4.19)$$

so  $\Theta$  is anti-linear and reverses the order of Grassmann factors. With the involution properties of  $\Xi$  (in particular  $\Xi^\top = \Xi$  and  $\Xi^2 = I$ ), one has  $\Theta^2 = \text{id}$  on  $\mathcal{A}_+^{\text{even}}$ . As before, the dot in  $\langle \Theta F \cdot F \rangle$  denotes the pointwise product in this graded algebra.

The map induced by  $\Theta$  on the set of Grassmann generators is a site permutation composed with an invertible linear transformation on the spin/internal indices with determinant  $\pm 1$ . In particular, it has unit Berezin Jacobian, and any global reordering sign is irrelevant on  $\mathcal{A}_+^{\text{even}}$ . Hence we have

$$D(\Theta\bar{\psi}) D(\Theta\psi) = D\bar{\psi} D\psi. \quad (4.20)$$

Together with the already established  $\Theta$ -invariance of  $Dx$ ,  $DU$ , and  $D\phi$ , the full product measure  $Dx DU D\phi D\bar{\psi} D\psi$  is  $\Theta$ -invariant at finite volume.

As in §3.1, we build fermion actions from local geometric data and finite stencils on the abstract lattice, and then apply the  $\theta$ -partner/averaging prescription to enforce  $\Theta$ -invariance. In particular, the averaged naive action (3.23) is local and has time-range one in the index-time direction.

As in the proof of Theorem 4.3, we decompose the extended field multiplet  $\omega = (x, U, \phi, \bar{\psi}, \psi)$  as  $\omega = (\omega_-, \omega_0, \omega_+)$  using a reflection slab  $\Sigma_\ell$  wide enough to contain the time-range  $\ell$  of the stencil. By finite time-range, no local term can simultaneously involve strict-past variables and strict-future variables; consequently one can (uniquely, up to regrouping purely  $\omega_0$  terms) write

$$S_f(\omega) = S_{f,+}(\omega_0, \omega_+) + S_{f,0}(\omega_0) + S_{f,-}(\omega_0, \omega_-), \quad S_{f,-} = \Theta S_{f,+}. \quad (4.21)$$

For fermions, locality and  $\Theta$ -invariance are not by themselves sufficient: the additional input is positivity of the *slab pairing* across the reflection plane, which we isolate next.

We say that a Grassmann-even fermion action  $S_f$  has a *reflection-positive slab form (of width  $\ell$ )* if the slab weight admits a finite “sum of  $\Theta$ -squares” representation

$$e^{-S_{f,0}(\omega_0)} = \sum_{j \in J} (\Theta B_j)(\omega_0) B_j(\omega_0), \quad B_j \in \mathcal{A}_+^{\text{even}} \text{ supported in } \Sigma_\ell \cap \Lambda_+, \quad (4.22)$$

for some finite index set  $J$ . (Finiteness is automatic since the Grassmann algebra on  $\Sigma_\ell$  is finite-dimensional and the exponential truncates.) Equivalently, it suffices to have a representation  $S_{f,0} = S_{f,0}^{\text{loc}} - \sum_k c_k (\Theta \chi_k) \chi_k$  with  $c_k \geq 0$  bosonic and  $\chi_k$  odd supported in  $\Sigma_\ell \cap \Lambda_+$ ; expanding the exponential then yields (4.22).

**Theorem 4.5.** *Let  $S_b = S_x + S_{\text{fields}}^{(\text{bos})}$  be the bosonic part of the action and let  $S_f$  be a Grassmann-even fermion action. Assume:*

- (i)  $S_b$  and  $S_f$  are local on the abstract lattice and have finite interaction range  $\ell < \infty$  in the index-time direction.
- (ii)  $S_b(\Theta\omega) = S_b(\omega)$  and  $S_f(\Theta\omega) = S_f(\omega)$ , and the hard constraint  $\mathcal{X}_{\text{adm}}$  and the product measures are  $\Theta$ -invariant (including (4.20)).
- (iii)  $S_f$  admits a reflection-positive slab form of width  $\ell$  in the sense of (4.21)–(4.22).

Then for all  $F \in \mathcal{A}_+^{\text{even}}$  one has

$$\langle \Theta F \cdot F \rangle \geq 0,$$

where  $\langle \cdot \rangle$  denotes expectation with respect to the joint finite-volume measure

$$1_{\{x \in \mathcal{X}_{\text{adm}}\}} e^{-S_b - S_f} Dx DU D\phi D\bar{\psi} D\psi.$$

*Proof.* As in Theorem 4.3, the finite time-range assumption implies a decomposition

$$S_b(\omega) = S_{b,+}(\omega_0, \omega_+) + S_{b,0}(\omega_0) + S_{b,-}(\omega_0, \omega_-), \quad S_{b,-} = \Theta S_{b,+}.$$

Combine this with (4.21) to obtain for the total action

$$S(\omega) = S_+(\omega_0, \omega_+) + S_0(\omega_0) + S_-(\omega_0, \omega_-), \quad S_- = \Theta S_+,$$

where  $S_0 = S_{b,0} + S_{f,0}$  depends only on  $\omega_0$ .

Let  $F \in \mathcal{A}_+^{\text{even}}$ , so  $F$  depends only on  $(\omega_0, \omega_+)$ . Define the (graded) conditional functional

$$\Psi_F(\omega_0) = \int e^{-S_+(\omega_0, \omega_+)} F(\omega_0, \omega_+) d\omega_+,$$

where  $d\omega_+$  includes the bosonic product measures and the Berezin factors over the  $\omega_+$  Grassmann generators. Using  $\Theta$ -invariance of the domain and product measures and the relation  $S_- = \Theta S_+$ , one obtains the standard factorization

$$\langle \Theta F \cdot F \rangle = \frac{1}{Z} \int e^{-S_0(\omega_0)} (\Theta \Psi_F)(\omega_0) \Psi_F(\omega_0) d\omega_0.$$

Now split  $e^{-S_0} = e^{-S_{b,0}} \cdot e^{-S_{f,0}}$  and use (4.22):

$$e^{-S_{f,0}} = \sum_{j \in J} (\Theta B_j) B_j.$$

Since  $\Psi_F$  is even and  $\Theta$  is an involution on the even algebra, the integrand becomes a finite sum of terms of the form

$$e^{-S_{b,0}(\omega_0)} (\Theta(B_j \Psi_F))(\omega_0) (B_j \Psi_F)(\omega_0),$$

each of which integrates to a nonnegative number by the defining property of a  $\Theta$ -square pairing on  $\mathcal{A}_+^{\text{even}}$ . Summing over  $j$  yields  $\langle \Theta F \cdot F \rangle \geq 0$ .  $\square$

**Example 4.6** (Geometric Wilson/projector mechanism). A standard sufficient mechanism for the slab-positivity condition (4.22) is that the couplings crossing the reflection plane factor through orthogonal projectors with *nonnegative* coefficients. In the present geometric setting, the natural constant projectors  $P_{\pm} = \frac{1}{2}(1 \pm \gamma_1)$  are replaced by the site-wise projectors built from (4.17):

$$P_{\pm}(n) := \frac{1}{2}(I \pm \Xi(n)), \quad P_{\pm}(n)^2 = P_{\pm}(n), \quad P_+(n)P_-(n) = 0.$$

Concretely, let  $V(n; x) > 0$  be a local scalar weight (e.g. a cell volume), let  $M(n; x) \in \mathbb{R}$  be an ultralocal mass weight, and let  $w_{\mu}(n; x) > 0$  be a local link weight attached to the oriented link  $(n, \mu)$ , all built from local Euclidean invariants of  $x$ . Consider a Wilson-type prototype action whose time-like hops are written directly in projector form:

$$S_W^{\circ}[x, U, \bar{\psi}, \psi] = \sum_{n \in \Lambda} V(n; x) \bar{\psi}(n) M(n; x) \psi(n) \tag{4.23}$$

$$- \sum_{n \in \Lambda} V(n; x) w_1(n; x) \bar{\psi}(n) P_-(n) U_1(n) \psi(n + \hat{1}) \tag{4.24}$$

$$- \sum_{n \in \Lambda} V(n; x) w_{-1}(n; x) \bar{\psi}(n) P_+(n) U_{-1}(n) \psi(n - \hat{1}) \tag{4.25}$$

+ (terms not crossing the reflection plane).

Here  $U_{-1}(n) = U_1(n - \hat{1})^{-1}$  as usual. The omitted terms may include arbitrary local spatial hops and on-slice couplings; they do not affect the slab pairing because they do not connect the two sides of the reflection plane.

Apply the  $\theta$ -partner/averaging prescription of §3.1 to obtain the averaged action  $S_W = \frac{1}{2}(S_W^\circ + S_W^q)$ , hence  $\Theta S_W = S_W$ . In the slab decomposition (4.21), the only fermionic terms that genuinely couple the two sides are the time-like hops across the reflected time link, and because they factor through  $P_\pm(n)$  with nonnegative coefficients, the corresponding slab weight admits a representation (4.22). Therefore  $S_W$  satisfies hypothesis (iii) of Theorem 4.5, and reflection positivity holds for all  $F \in \mathcal{A}_+^{\text{even}}$ .

### 4.3 Symanzik effective theory and universality

The purpose of this section is to make precise (at the level customary in lattice EFT) the statement that DLR defines a *local* regulator with *exact*  $\text{SE}(d)$  symmetry, and that it belongs to the same universality class as the corresponding theory on a rigid hypercubic lattice, under a mild short-range hypothesis for the geometry sector.

Fix a matter content (scalar, gauge, fermion) and consider the DLR partition function

$$Z(a) = \int_{\mathcal{X}_{\text{adm}}(a)} Dx \int DU \int D\Phi \exp(-S_x[x] - S_{\text{fields}}[x, U, \Phi]). \quad (4.26)$$

Because the underlying graph is fixed and the admissibility conditions are local, the DLR action is ultralocal in the abstract lattice coordinates and has a standard transfer-matrix interpretation once a reflection direction is chosen. In particular, for any local observable of the enlarged theory supported on a bounded region, the dependence on distant lattice sites enters only through local propagation. For the universality questions of interest here we focus on observables depending only on the gauge/matter fields  $(U, \Phi)$ ; geometry observables probe the regulator sector itself.

Symanzik effective field theory is a convenient way to parameterize *lattice artifacts* in long-distance observables, cf. [16, 17]. Concretely, one considers correlation functions of local operators at a *fixed physical separation*  $|x|$  while taking the cutoff  $a \rightarrow 0$ . On the lattice this means that the separation in lattice units grows as  $r = |x|/a \rightarrow \infty$ , so the correlators probe distances that are large compared to the cutoff but still finite in physical units.

Under the standard assumptions of locality and a mass gap at the cutoff scale, the effect of the regulator at such distances can be encoded by a continuum effective action

$$S_{\text{eff}} = S_{\text{cont}} + \sum_i a^{\Delta_i} c_i(g_{\text{bare}}) \mathcal{O}_i, \quad (4.27)$$

where  $\{\mathcal{O}_i\}$  is a basis of local continuum operators (composite operators built from the fields and their derivatives) and  $\Delta_i > 0$  are their excess dimensions relative to the target action. The coefficients  $c_i(g_{\text{bare}})$  are *matching coefficients*: they depend on the microscopic definition of the regulator (hence on the bare couplings  $g_{\text{bare}}$ ) and are generally scheme-dependent, but the operator basis is *not* arbitrary. Indeed, the allowed operators  $\mathcal{O}_i$  are precisely those compatible with the *exact* symmetries of the regulator.

In particular, on a rigid hypercubic lattice the exact symmetry is only the hypercubic group  $\text{H}(d)$ , so the Symanzik operator basis is larger than the  $\text{SO}(d)$ -scalar basis and radiative corrections can generate *rotation-breaking* higher-derivative terms. For a scalar field, writing  $H_{\mu\nu} = \partial_\mu \partial_\nu \phi$ , the  $\text{SO}(d)$ -invariants at four-derivative order are  $\text{tr}(H)^2 = (\partial^2 \phi)^2$  and  $\text{tr}(H^2) = \sum_{\mu,\nu} (\partial_\mu \partial_\nu \phi)^2$ . By



contrast, hypercubic symmetry permits independent coefficients for the diagonal and off-diagonal pieces, e.g.,  $\sum_{\mu}(\partial_{\mu}^2\phi)^2$  and  $\sum_{\mu<\nu}(\partial_{\mu}\partial_{\nu}\phi)^2$ . Reducing  $\text{SO}(d)$  to  $\text{H}(d)$  enlarges the allowed mixing among operators with the same quantum numbers, permitting additional anisotropic counterterms that are absent for an  $\text{SO}(d)$ -covariant regulator.

The only additional assumption needed to reduce DLR to an ordinary Symanzik problem is:

**Hypothesis 4.7** (Short-range geometry). After quotienting by the global  $\text{SE}(d)$  zero modes, connected correlation functions of local geometric observables (built from finitely many  $e_{\mu}(n)$ ,  $g_{\mu\nu}(n)$ ,  $V(n)$ , etc.) decay exponentially in lattice distance, uniformly in  $a$ , i.e. the geometry sector has a finite correlation length in lattice units.

This hypothesis is a genuine condition on the geometry measure and therefore constrains the admissible choices of  $S_x$ . A natural way to target (SR) is to include an explicit local stiffness scale for the embedding fluctuations (e.g. quadratic penalties around a reference metric as in (2.21)), which makes the non-zero-mode fluctuations of  $x(n) = an + \eta(n)$  effectively massive in lattice units. The hard admissibility constraints are compatible with such a massive regime and help by excluding degenerate cells, but by themselves they do not guarantee a mass gap or exponential mixing. This distinction is particularly important in higher dimensions, where entropic instabilities of random geometry ensembles are well known. Accordingly, we treat (SR) as an explicit assumption to be verified for any proposed  $S_x$ , and we include direct diagnostics in Section 5. In  $d = 2$  we find behaviour consistent with a short-range twisting regime; however the  $d = 4$  situation remains to be mapped.

Assuming (SR), one may integrate out the geometry field at fixed  $a$  to obtain an effective action for the field sector  $(U, \Phi)$  alone. Locality and (SR) imply that this effective action is local and admits a Symanzik expansion of the form (4.27). Moreover, because the DLR measure is  $\text{SE}(d)$ -covariant, the induced effective action for  $(U, \Phi)$  is  $\text{SO}(d)$ -covariant, and gauge invariant when gauge fields are present. In particular, only  $\text{SO}(d)$ -scalar operators contribute to scalar observables. This removes the representation-theoretic source of rotation-breaking counterterms and, more importantly, potentially simplifies Symanzik improvement and operator renormalisation: the basis of allowed counterterms (and hence the pattern of operator mixing) is constrained by full  $\text{SO}(d)$  rather than only the hypercubic group.

Crucially, integrating out short-range geometry changes the *relation* between bare and renormalized parameters. Concretely, averaging the local volume/metric factors over  $x$  produces finite (scheme-dependent) shifts in the coefficients of the operators already present in the target continuum theory—e.g. the mass term, the kinetic normalization, and (when present) the bare quartic or gauge coupling. This is the usual regulator dependence of the bare-to-renormalized map and simply means that the critical surface and tuning relations  $g_{\text{bare}}(a)$  are modified. What short-range geometry *cannot* do is generate new relevant or marginal operators not already allowed by the continuum symmetries: that would require additional light degrees of freedom or genuinely long-range interactions in the geometry sector, which are excluded by (SR).

**Remark 4.8.** One might wonder whether the benefits of exact  $\text{SO}(d)$  covariance at nonzero cutoff could be obtained more economically by adding a single global rotation variable  $R \in \text{SO}(d)$  to an ordinary hypercubic lattice, i.e., by considering an embedding  $x_R(n) = aRn$  and averaging over  $R$ . Viewed as a “geometry sector”, this degree of freedom is maximally long-range: local geometric observables built from  $e_{\mu}$ ,  $g_{\mu\nu}$ ,  $V$  are perfectly correlated across the lattice, so the short-range hypothesis (SR) fails in the strongest possible way.

In standard hypercubic LGT this construction is nevertheless trivial, because the action depends only on the abstract graph and fixed hypercubic coefficients and is independent of the embedding: the integral over  $R$  merely multiplies the partition function by  $\text{Vol}(\text{SO}(d))$  and, after “integrating out”  $R$ , one simply recovers the usual hypercubic theory. In particular, the Symanzik operator basis remains that of the hypercubic regulator. On a finite periodic torus the situation is even more restrictive: a generic rotation does not preserve the period lattice and therefore does not define a symmetry of the discrete torus beyond its discrete hypercubic subgroup.

By contrast, DLR integrates over a *local* embedding field  $x(n)$  that enters the action through local metric/volume factors. After quotienting by (or fixing) the global  $\text{SE}(d)$  zero modes to remove the infinite group volume, the geometry still fluctuates locally. Assuming (SR), integrating out  $x$  produces a *local* effective action for  $(U, \Phi)$  to which the Symanzik expansion applies, and the underlying  $\text{SE}(d)$  covariance implies that the induced effective action is globally  $\text{SO}(d)$ -covariant.

A purely global “geometry” variable (such as a rigid rotation) has infinite correlation length; if it were coupled nontrivially it would act as a mediator producing nonlocal effective interactions upon elimination, which lies outside the scope of the Symanzik expansion and is exactly what (SR) excludes.

To connect the Symanzik discussion to the usual perturbative intuition, expand the embedding about the regular one,

$$x(n) = a n + \eta(n), \quad e_\mu(n) = x(n + \hat{\mu}) - x(n) = a \hat{\mu} + \delta e_\mu(n), \quad (4.28)$$

where  $\delta e_\mu(n) = \eta(n + \hat{\mu}) - \eta(n)$  and  $\eta(n) \in \mathbb{R}^d$ . Throughout this and the next subsections,  $\nabla_\mu$  denotes the forward lattice derivative

$$(\nabla_\mu f)(n) = \frac{f(n + \hat{\mu}) - f(n)}{a}, \quad (4.29)$$

acting componentwise on  $\mathbb{R}^d$ -valued fields. In particular,

$$(\nabla_\mu \eta)(n) = \frac{\eta(n + \hat{\mu}) - \eta(n)}{a} = \frac{\delta e_\mu(n)}{a} \in \mathbb{R}^d. \quad (4.30)$$

Heuristically, if  $\eta(n) = u(an)$  for a smooth interpolant  $u$ , then  $\nabla_\mu \eta(n) = \partial_\mu u(an) + O(a)$ .

Fix components with respect to the regular orthonormal frame  $\{\hat{\mu}\}$ :

$$\eta_\nu(n) = \hat{\nu} \cdot \eta(n), \quad (\nabla \eta)_{\mu\nu}(n) = \nabla_\mu \eta_\nu(n). \quad (4.31)$$

Thus  $\nabla \eta$  is the lattice Jacobian, its trace

$$\nabla \cdot \eta(n) = \text{tr}(\nabla \eta)(n) = \sum_\mu \nabla_\mu \eta_\mu(n), \quad (4.32)$$

is the discrete divergence, and we write  $|\nabla \eta|^2 = \sum_{\mu,\nu} (\nabla_\mu \eta_\nu)^2$  for the canonical  $\text{SO}(d)$ -scalar quadratic in first differences. When writing schematic vertices such as  $(\nabla \eta)(\nabla \phi)(\nabla \phi)$ , indices are understood to be contracted in an  $\text{SO}(d)$ -covariant way.

On the periodic torus we use the backward derivative  $(\nabla_\mu^* f)(n) = (f(n) - f(n - \hat{\mu}))/a$  and the associated backward gradient  $(\nabla^* F)_\mu = \nabla_\mu^* F$ . Then for any scalar  $F$ , we have

$$\sum_n (\nabla \cdot \eta)(n) F(n) = - \sum_n \eta(n) \cdot (\nabla^* F)(n), \quad (4.33)$$

with no boundary term on the torus.

All local geometric data entering the field actions are smooth local functions of  $\nabla\eta(n)$ , more precisely of the frame matrix  $E(n)$  built from the  $e_\mu(n)$ . Expanding around the regular embedding therefore yields schematic local expansions

$$g_{\mu\nu}(n) = a^2(\delta_{\mu\nu} + O(\nabla\eta)), \quad V(n) = a^d(1 + O(\nabla\eta) + O(|\nabla\eta|^2)), \quad (4.34)$$

with coefficients bounded uniformly on  $\mathcal{X}_{\text{adm}}$  by admissibility (uniform shape regularity).

Let us consider the scalar  $\phi^4$  theory for definiteness. Writing the scalar action on a general admissible geometry as  $S_\phi[x, \phi] = S_\phi^{(0)}[\phi] + S_{\phi\eta}^{(1)}[\phi, \eta] + S_{\phi\eta}^{(2)}[\phi, \eta] + \dots$ , we see that the regular-lattice part  $S_\phi^{(0)}$  is the usual hypercubic action, while the geometry-dependent pieces split into two distinct families already at first order, as follows.

(i) *Metric-induced (kinetic) couplings.* Expanding the factor  $V g^{\mu\nu}$  multiplying discrete derivatives produces vertices bilinear in  $\phi$ , schematically of the form

$$\begin{aligned} S_{\phi\eta}^{(1)} &\supset \sum_n a^d (\nabla\eta)(n) (\nabla\phi)(n) (\nabla\phi)(n), \\ S_{\phi\eta}^{(2)} &\supset \sum_n a^d |\nabla\eta(n)|^2 (\nabla\phi)^2(n), \end{aligned} \quad (4.35)$$

and higher orders. These are the ‘‘derivative bilinear’’ couplings.

(ii) *Volume-induced (potential) couplings.* The volume factor  $V(n)$  multiplies the mass and quartic densities. At linear order its variation is a scalar made from  $\nabla\eta$  (indeed a discrete divergence), so the expansion produces vertices with *no* derivatives on  $\phi$ :

$$\begin{aligned} S_{\phi\eta}^{(1)} &\supset \sum_n a^d (\nabla \cdot \eta)(n) \left( \frac{1}{2} m_0^2 \phi(n)^2 + \frac{\lambda_0}{4!} \phi(n)^4 \right), \\ S_{\phi\eta}^{(2)} &\supset \sum_n a^d |\nabla\eta(n)|^2 (\phi^2 + \phi^4). \end{aligned} \quad (4.36)$$

On the periodic torus (or with suitable decay), the linear volume variation is the trace of the lattice Jacobian, so schematically

$$V(n) = a^d \left( 1 + \nabla \cdot \eta(n) + O(|\nabla\eta|^2) \right). \quad (4.37)$$

Thus the first-order potential contribution includes, in particular, the quartic term

$$\sum_n a^d (\nabla \cdot \eta)(n) \frac{\lambda_0}{4!} \phi(n)^4. \quad (4.38)$$

Applying (4.33) with  $F = \phi^4$  gives

$$\sum_n (\nabla \cdot \eta)(n) \phi(n)^4 = - \sum_n \eta(n) \cdot \nabla^*(\phi^4)(n), \quad (4.39)$$

on the torus. Hence even the non-derivative  $\phi^4$  term arising from the volume factor may be rewritten as a coupling of  $\eta$  to a lattice derivative of a local density. Equivalently, since  $x$  enters the microscopic action only through differences  $e_\mu(n)$ , the fluctuation field has the shift symmetry

$\eta \mapsto \eta + c$ , so every  $\eta$  insertion carries at least one lattice derivative (and therefore a factor of  $\hat{p}$  in momentum space).

Assuming (SR), connected correlators of local geometric observables built from finitely many  $\nabla\eta$ ,  $g_{\mu\nu}$ ,  $V$ , etc. decay exponentially in lattice distance, uniformly in  $a$ . Equivalently, the geometry sector has a finite correlation length in lattice units, hence a mass scale of order  $1/a$  in physical units. As a result, integrating out  $\eta$  at fixed  $a$  produces a *local* effective action for the field sector  $(U, \Phi)$ , with a derivative expansion in powers of  $pa$  at fixed physical external momenta  $p$ . This is precisely the input needed for the Symanzik description: all induced operators are local and, by  $SE(d)$  covariance of the regulator, transform covariantly under  $SO(d)$ , and are gauge invariant when gauge fields are present. The geometry sector can and will renormalize the *bare-to-renormalized map* (shifting masses/couplings and wave-function normalizations), and it can generate higher-dimension  $SO(d)$ -scalar operators (including higher-point operators such as  $\phi^6, \phi^8, \dots$ ), but under (SR) it cannot produce new relevant/marginal operators beyond those allowed by the target continuum symmetries.

This motivates the following universality statement.

**Conjecture 4.9.** Assume (SR) and fix/quotient the global  $SE(d)$  zero modes in an  $SE(d)$ -covariant manner (so that local correlators are affected only by finite-volume effects). Then, for any choice of local field content  $(U, \Phi)$  and any local  $SE(d)$ -covariant discretization of the corresponding continuum action, the DLR defines a local effective field theory for  $(U, \Phi)$  whose long-distance correlators admit a Symanzik expansion (4.27) with the following properties:

- (i) The induced Symanzik operators  $\mathcal{O}_i$  may be chosen to be gauge invariant (when gauge fields are present) and to transform covariantly under  $SO(d)$ ; in particular, only  $SO(d)$ -scalar operators contribute to scalar observables. Consequently, the set of allowed counterterms and the pattern of operator mixing are constrained by full  $SO(d)$ , rather than only the hypercubic symmetry.
- (ii) Integrating out the short-range geometry modifies the relation between bare and renormalized parameters: the critical surface and the tuning relations  $g_{\text{bare}}(a)$  may shift compared with a rigid hypercubic regulator. However, no new relevant or marginal directions are generated beyond those already allowed by the target continuum symmetries.
- (iii) After tuning the usual relevant parameters (e.g. the mass in scalar theories, and the gauge coupling in gauge theories), the continuum limit of DLR lies in the same universality class as the corresponding continuum QFT. Equivalently, all continuum correlation functions of renormalized local observables agree with those obtained from any other local regulator preserving the same internal symmetries.

In particular, for scalar  $\phi^4$  theory in  $d = 4$ , the coefficient of the one-loop  $\beta$ -function is unchanged by the geometry sector: geometry fluctuations can renormalize the mapping between  $\lambda_0$  and  $\lambda_R$ , but do not modify the universal one-loop running of  $\lambda_R$  (see §4.4).

At a conceptual level, Conjecture 4.9 is an application of EFT to the enlarged system  $(x, U, \Phi)$ . Exact  $SE(d)$  covariance of the microscopic measure implies that any effective action obtained after integrating out  $x$  is  $SO(d)$ -covariant (and gauge invariant when applicable), yielding (i). The substantive input is the short-range geometry hypothesis (SR): exponential clustering in the geometry sector gives a finite correlation length in lattice units, so integrating out  $x$  at fixed cutoff produces

a local effective action for  $(U, \Phi)$  admitting a derivative expansion in powers of  $pa$ . Consequently the geometry sector can only renormalize the matching of operators already present in the target theory and generate higher-dimension  $\text{SO}(d)$ -covariant operators suppressed by powers of  $a$ , giving (ii); standard RG universality then yields (iii) after tuning the usual relevant parameters. Conjecture 4.9 is intended as a concrete target for future work; establishing or falsifying it beyond one loop and in  $4d$  gauge theories would be particularly valuable.

#### 4.4 Example: one-loop $\beta$ -function in scalar $\phi^4$ theory

We illustrate Conjecture 4.9 on a test theory where the universal running is visible already at one loop: a real scalar  $\phi^4$  model in  $d = 4$  with local potential

$$V(\phi) = \frac{1}{2}m_0^2\phi^2 + \frac{\lambda_0}{4!}\phi^4, \quad (4.40)$$

discretised on the dynamical mesh as in Section 3. On the regular embedding  $x_{\text{reg}}(n) = an$  this reduces to the standard nearest-neighbour lattice discretisation. Write

$$x(n) = an + \eta(n), \quad (4.41)$$

and assume the short-range geometry hypothesis (SR) from §4.3: connected correlators of local geometric observables built from finitely many  $e_\mu(n)$ ,  $g_{\mu\nu}(n)$ ,  $V(n)$  decay exponentially in lattice distance, uniformly in  $a$ . Equivalently (and this is how it is used perturbatively), the  $\eta$ -sector has a finite correlation length in lattice units. In physical units this means the geometry modes are *heavy* with characteristic mass scale  $\sim 1/a$ , so integrating them out produces a local effective lattice theory for  $\phi$  whose induced interactions are short-range and analytic in the external momenta at scales  $\mu \ll 1/a$ .

As discussed previously, expanding the scalar action  $S_\phi[x, \phi]$  in powers of  $\nabla\eta$  produces two conceptually different classes of geometry-matter couplings.

- *Kinetic (metric/frame) vertices.* Expanding  $V(n)g^{\mu\nu}(n)\nabla_\mu\phi\nabla_\nu\phi$  generates vertices where geometry couples to *derivative bilinears* in  $\phi$ , schematically

$$(\nabla\eta)(\nabla\phi)(\nabla\phi), \quad |\nabla\eta|^2(\nabla\phi)(\nabla\phi), \dots \quad (4.42)$$

These are the vertices that contribute to wave function renormalisation and to higher-derivative Symanzik operators.

- *Volume vertices.* Expanding the local volume factor  $V(n)$  in

$$\sum_n V(n) \left( \frac{1}{2}m_0^2\phi(n)^2 + \frac{\lambda_0}{4!}\phi(n)^4 \right) \quad (4.43)$$

produces vertices with no derivatives on the scalar legs (though every  $\eta$  insertion carries at least one lattice derivative), e.g.

$$(\nabla \cdot \eta) \phi^2, \quad (\nabla \cdot \eta) \phi^4, \quad |\nabla\eta|^2 \phi^2, \quad |\nabla\eta|^2 \phi^4, \dots \quad (4.44)$$

What matters for universality is that under (SR) these vertices describe couplings to a heavy, short-range field.

The one loop renormalisation of the quartic coupling is determined by the coefficient of the logarithmic dependence on the renormalisation scale  $\mu$  in the amputated 1PI four–point function. This coefficient is universal: it arises from the loop–momentum window *above*  $\mu$  but *below* the cutoff (heuristically  $\mu \ll |k| \ll 1/a$ ), and is insensitive to finite, scheme–dependent redefinitions of bare parameters.

(A) *Pure scalar bubble.* The one–loop 1PI four–point graphs built only from the usual  $\phi^4$  vertex are exactly those of the static hypercubic lattice (the *s/t/u* bubbles), cf. Fig. 1a. In each channel there are *two* internal scalar propagators running in the loop, hence the characteristic integrand  $(\hat{k}^2 + m_0^2)^{-2}$ . In particular, the standard bubble integral yields

$$I_{\text{lat}}(a, m_0) = \int_B \frac{d^4k}{(2\pi)^4} \frac{1}{(\hat{k}^2 + m_0^2)^2} = \frac{1}{16\pi^2} \log \frac{1}{a^2 m_0^2} + \text{finite}, \quad (4.45)$$

and summing the three channels produces the familiar one–loop coefficient  $3/(16\pi^2)$  in the  $\phi^4$  channel. Here  $B = [-\pi/a, \pi/a]^4$  is the Brillouin zone and

$$\hat{k}_\mu = \frac{2}{a} \sin\left(\frac{ak_\mu}{2}\right), \quad \hat{k}^2 = \sum_{\mu=1}^4 \hat{k}_\mu^2, \quad (4.46)$$

so that the free lattice propagator is  $(\hat{k}^2 + m_0^2)^{-1}$ .

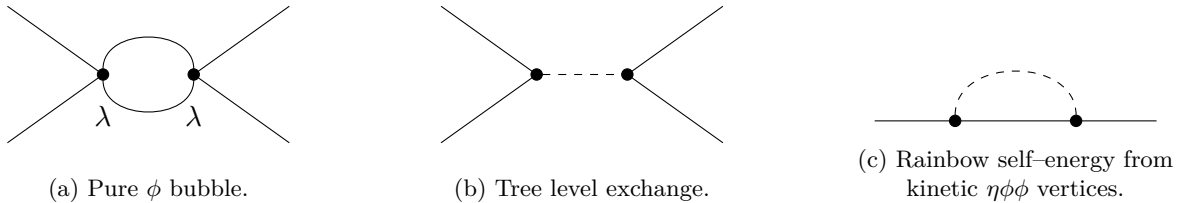


Figure 1: Building blocks in the perturbative universality argument. Solid:  $\phi$ . Dashed:  $\eta$ .

(B) *Diagrams with internal geometry lines.* At one loop, any 1PI four–point contribution that involves at least one internal  $\eta$  propagator is controlled by (SR). Indeed, (SR) implies the  $\eta$  correlator decays exponentially in lattice units, so the geometry is massive in lattice units. Consequently, at external scales  $\mu \ll 1/a$ , graphs with internal  $\eta$  lines generate *local* contributions analytic in the external momenta:

- *Kinetic vertices.* Kinetic vertices necessarily carry external momenta: already at tree level, two  $\eta\phi\phi$  vertices connected by a single internal  $\eta$  line produce a momentum–dependent 4–point amplitude (Fig. 1b), whose low–energy expansion generates higher–derivative operators in the Symanzik action, not a momentum–independent shift of the  $\phi^4$  coupling. The corresponding 2–point correction is the rainbow self–energy in Fig. 1c.
- *Volume vertices.* These can and do renormalise the *bare-to-renormalised map*: integrating out short–range volume fluctuations shifts the coefficients of operators already present in the target theory (mass term, kinetic normalisation, and the quartic coupling) by finite, scheme–dependent amounts (Fig. 2a). In addition, exchanging a short–range  $\eta$  line between two local volume insertions produces higher multi–field operators; for example Fig. 2b corresponds to an induced  $\phi^8$  interaction, which is irrelevant in  $d = 4$  and does not affect the running of  $\lambda$ . Neither mechanism can generate a new logarithmic  $\mu$ –dependence in the  $\phi^4$  channel at one loop.

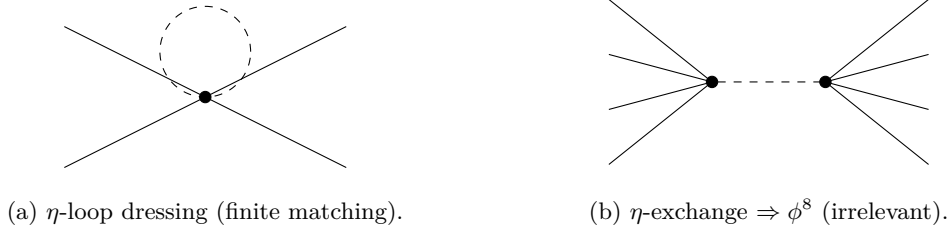


Figure 2: Further one-loop graphs with internal geometry lines (line conventions as in Fig. 1).

Assume (SR), so the  $\eta$ -propagator has a mass scale of order one in lattice units. At external scales  $\mu \ll 1/a$ , any 1PI graph with at least one internal  $\eta$  line produces a local contribution analytic in the external momenta. Consequently, kinetic vertices contribute only to wave-function renormalisation and higher-derivative operators, while volume vertices can shift the local  $\phi^4$  coefficient by a finite (scheme-dependent) amount and can induce irrelevant multi-field operators (e.g. Fig. 2b), but cannot generate an additional  $\log \mu$  term in the  $\phi^4$  channel at one loop. Therefore the coefficient of the logarithmic divergence in the  $\phi^4$  channel is entirely due to the pure scalar bubbles and equals  $3/(16\pi^2)$ , as stated in (4.47); after the usual field renormalisation the renormalised quartic coupling  $\lambda(\mu)$  obeys the same one-loop renormalisation-group equation as in the continuum and in the static-lattice regularisation,

$$\mu \frac{d\lambda}{d\mu} = \beta(\lambda) = \frac{3}{16\pi^2} \lambda^2 + O(\lambda^3), \quad (4.47)$$

while the dynamical geometry affects only finite matching and higher-dimension operators in the Symanzik expansion. This supports Conjecture 4.9.

## 5 Numerical experiments

This section describes the Monte Carlo setup and numerical diagnostics used to test the dynamical-lattice regulator (DLR) in a two-dimensional scalar theory. The goal is proof-of-concept rather than high-precision spectroscopy: we check (i) algorithmic viability under standard local updates, (ii) that the geometry sector remains massive near matter criticality (the short-range geometry hypothesis (SR)), (iii) suppression of direction-dependent cutoff artefacts at finite lattice spacing, and (iv) preservation of long-distance universality in a standard finite-size scaling test.

A central working assumption is the short-range geometry hypothesis (SR). In the numerics below we treat (SR) as a stringent diagnostic: even when the scalar is tuned close to criticality, the geometry should not develop long range modes.

Throughout, *baseline* refers to the fixed regular square lattice, while *dynamical* refers to the coupled geometry-scalar system in which the embedding  $x : \Lambda \rightarrow \mathbb{R}^2$  is updated alongside the matter field.

### 5.1 Simulation protocol

We work on a periodic  $L \times L$  abstract lattice  $\Lambda = \{0, \dots, L-1\}^2$  with lattice spacing  $a = 1$  unless stated otherwise. The dynamical degrees of freedom are an embedding  $x(n) \in \mathbb{R}^2$  and a real scalar

field  $\phi(n) \in \mathbb{R}$  at each  $n \in \Lambda$ . The joint Boltzmann weight is

$$Z^{-1} \exp(-S_x[x] - S_\phi[x, \phi]), \quad Dx D\phi = \prod_{n \in \Lambda} d^2x(n) d\phi(n),$$

with  $x$  restricted to the admissible set  $\mathcal{X}_{\text{adm}}$  of §2.2. The geometry action  $S_x$  is the local,  $E(2)$ -invariant action of §2.3, while the scalar action  $S_\phi$  is taken to be the *prototype* action  $S_\phi = S_\phi^\circ$  of §3.1 (i.e. before  $\theta$ -averaging), evaluated on the same embedded mesh, with the local potential

$$W_{\text{loc}}(\phi) = \frac{1}{2}\mu^2\phi^2 + \lambda\phi^4. \quad (5.1)$$

Note that the theory is parametrized by the bare couplings  $(\mu^2, \lambda)$  in lattice units. Our simulation convention for the quartic term is  $\lambda\phi^4$  (no  $1/4!$  factor). Thus, relative to the continuum-style normalization  $W_{\text{loc}}(\phi) = \frac{1}{2}m_0^2\phi^2 + \frac{\lambda_0}{4!}\phi^4$  used before, we have

$$m_0^2 = \mu^2, \quad \lambda_0 = 24\lambda.$$

We set  $\lambda = 1$  and vary  $\mu^2$  in the universality tests, while we use  $\lambda = 0.1$  and  $\mu^2 = 1$  for all other experiments.

*Periodic geometry.* The physical domain is a flat torus with period vectors  $P_0 = (La, 0)$  and  $P_1 = (0, La)$ . We store  $x(n)$  in a fixed fundamental domain  $[0, La) \times [0, La)$  and use a minimal-image convention for displacements: whenever a neighbour crosses the boundary we shift by integer multiples of  $P_0, P_1$  to obtain the shortest representative. All geometric quantities are computed cellwise from the four vertices of a plaquette, using this periodic reconstruction.

This convention fixes the fundamental cycles of the physical torus in finite volume. All diagnostics below are phrased in terms of local twisting/mixing and connected correlators, hence are insensitive to the particular representative chosen for the global  $SE(2)$  zero modes.

*Local admissibility.* Each cell is required to be convex and shape-regular. Concretely, for the numerical runs we impose the fixed local bounds

$$A \geq A_{\min} = 0.10, \quad \ell_\mu \leq \ell_{\max} = 4.0, \quad \text{aspect} \leq R_{\max} = 4.0, \quad 30^\circ \leq \vartheta \leq 150^\circ,$$

where  $\ell_\mu$  are the two edge lengths,  $A$  is the cell area,  $\vartheta$  is the corner angle between the two edges, and  $\text{aspect} = \max(\ell_1, \ell_2) / \min(\ell_1, \ell_2)$ . The specific numerical values are not tuned: they are conservative bounds chosen to exclude near-degenerate cells while allowing broad fluctuations away from the regular embedding. Moves that violate any bound on any affected cell are rejected immediately. In practice these hard constraints prevent near-degenerate cells and keep the simulation in the same connected component as the regular embedding.

*Updates.* Both geometry and scalar field sweeps use local Metropolis proposals at uniformly chosen sites.

- *Geometry move:* pick  $n \in \Lambda$  and propose  $x'(n) = x(n) + \varepsilon_x$  with  $\varepsilon_x \sim \text{Unif}([-\Delta_x, \Delta_x]^2)$ , wrapped back into the fundamental domain. The move changes only the four cells adjacent to  $n$ ; we re-evaluate their admissibility and their local contributions to  $S_x$  and  $S_\phi$ , and accept with probability  $\min\{1, \exp(-\Delta S_x - \Delta S_\phi)\}$ .
- *Scalar move:* pick  $n \in \Lambda$  and propose  $\phi'(n) = \phi(n) + \varepsilon_\phi$  with  $\varepsilon_\phi \sim \text{Unif}[-\Delta_\phi, \Delta_\phi]$ . Only the four adjacent cells change; we accept with probability  $\min\{1, \exp(-\Delta S_\phi)\}$ .



We distinguish a *geometry sweep* and a *scalar sweep*, each consisting of  $L^2$  single-site proposals of the corresponding type. One Monte Carlo *cycle* comprises one geometry sweep followed by one scalar sweep. Proposal scales are tuned to give  $O(1)$  acceptance rates; in the runs shown the geometry acceptance is typically in the few  $\times 10\%$  to  $\sim 80\%$  range, depending on  $(L, \mu^2)$ .

*Geometry action parameters.* For the numerical experiments we use a quadratic “spring” that penalizes only corner-angle distortions:

$$S_x[x] = \sum_{n \in \Lambda} \frac{k}{2} (\vartheta(n) - \vartheta_{\text{ref}})^2. \quad (k = 2.5).$$

Edge lengths, areas, and aspect ratios are controlled primarily by the hard admissibility constraints.

This minimal choice is designed to keep the geometry disordered at the level of local orientations while the hard constraints control degeneracies; it is *not* intended as an optimized  $S_x$  for  $d = 4$ .

*Run lengths.* For each parameter point we thermalise for  $N_{\text{therm}}$  sweeps (typically  $5 \times 10^3$ ), then record  $N_{\text{prod}}$  sweeps (typically  $2 \times 10^4$ ), storing measurements every  $k$  sweeps (typically  $k = 10$ ). Each experiment is repeated over a few dozen independent random seeds, and the same protocol is used uniformly across the  $(L, \mu^2)$  scan underlying the finite-size scaling plots.

## 5.2 Measured observables

We record both “health” diagnostics to monitor stability and mixing, and physics observables to compare baseline vs dynamical and to probe universality and rotational artefacts.

*Basic diagnostics.* On each measurement we record  $S_x$ ,  $S_\phi$ , the minimum/maximum cell area, and the maximum aspect ratio over the lattice. For the scalar we record the moments  $\langle \phi^2 \rangle = L^{-2} \sum_n \phi(n)^2$  and  $\langle \phi^4 \rangle = L^{-2} \sum_n \phi(n)^4$ .

*Geometry short-range diagnostics.* A key requirement is that the geometry acts as a regulator rather than an additional critical field (“SR hypothesis”). To test this we measure a connected volume-volume correlator built from the cell areas  $A(n)$ . On each stored configuration we form  $\delta A(n) = A(n) - \bar{A}$  with  $\bar{A} = |\Lambda|^{-1} \sum_m A(m)$ , and define the translation-averaged correlator

$$C_V(m) = \frac{1}{|\Lambda|} \sum_{n \in \Lambda} \delta A(n) \delta A(n+m),$$

where addition is modulo  $L$  in each direction. The reported  $C_V(m)$  is then the Monte-Carlo average of this quantity. We radially bin by the periodic graph ( $\ell^1$ ) distance

$$r(m) = \min(i, L-i) + \min(j, L-j)$$

for  $m = (i, j)$  and report

$$C_V(r) = \frac{1}{N_r} \sum_{m: r(m)=r} C_V(m), \quad N_r = \#\{m : r(m) = r\}.$$

In plots we show  $|C_V(r)|$  on a log scale and extract an effective decay length from an exponential fit over short to intermediate  $r$ .

*Short-distance rotational probe.* We measure an angle-binned finite-difference gradient observable: for a fixed list of short offsets  $\Delta$  (nearest neighbours, diagonals, and a few second neighbours),

we compute the minimal–image displacement  $v$ , its length  $\ell = |v|$ , and accumulate  $(\Delta\phi/\ell)^2$  into  $N_\theta = 18$  bins in  $[0, \pi)$  by the orientation of  $v$  (with  $v \sim -v$ ). From the resulting profile  $H(\theta) = \langle (\Delta\phi/\ell)^2 \rangle(\theta)$  we form the anisotropy measures

$$A_{\text{rms}} = \frac{\sqrt{\langle (H(\theta) - \bar{H})^2 \rangle_\theta}}{\bar{H}}, \quad A_4 = \frac{\sqrt{C_4^2 + S_4^2}}{\bar{H}},$$

with  $\bar{H} = \langle H(\theta) \rangle_\theta$ ,  $C_4 = \langle H(\theta) \cos 4\theta \rangle_\theta$ ,  $S_4 = \langle H(\theta) \sin 4\theta \rangle_\theta$ .

*Two–point functions and directional splitting.* We also measure a radial two–point function  $G(r)$  by choosing  $N_{\text{src}}$  random sources per measurement and correlating with all sites using minimal–image physical distances  $r = |x(n) - x(m)|$ , binned into  $N_r$  radial bins. To sharpen rotational artefact detection, we additionally measure direction–restricted correlators  $G_{\text{axis}}(r)$  and  $G_{\text{diag}}(r)$  from the same source–sink pairs by selecting displacements within  $\pm 15^\circ$  of the coordinate axes or diagonals. We plot both the correlators and their difference  $\Delta G(r) = G_{\text{diag}}(r) - G_{\text{axis}}(r)$ , which isolates the residual axial/diagonal splitting.

*Universality observables.* To locate the critical point and check the universality class we compute: (i) the Binder cumulant  $U_4 = 1 - \langle M^4 \rangle / (3\langle M^2 \rangle^2)$  with  $M = \sum_n \phi(n)$ , where  $\langle \cdot \rangle$  denotes the Monte Carlo average at fixed bare parameters; and (ii) the second–moment correlation length  $\xi$  from standard structure factor ratios, plotted as  $\xi/L$ . (Implementation details of the  $\xi$  estimator are standard and follow the usual periodic–torus definitions.)

### 5.3 Geometry sector diagnostics

Figure 3a shows a representative embedded mesh from the dynamical ensemble, illustrating that the geometry is genuinely fluctuating while remaining well inside the admissible region.

To quantify mesh fluctuations we show histograms of corner angles ( $\theta$ ) in Fig. 3b, edge lengths ( $\ell$ ) in Fig. 3c, cell areas ( $A$ ) in Fig. 3d, aspect ratios ( $r$ ) in Fig. 3e, and physical edge orientations in Fig. 3f. In lattice units we find (mean  $\pm$  standard deviation)

$$\langle \ell \rangle = 1.10 \pm 0.48, \quad \langle \theta \rangle = (86.7 \pm 27.1)^\circ, \quad \langle r \rangle \approx 1.78.$$

The distributions are broad (the mesh is not frozen near the square embedding) but show no visible pile–up at the admissibility cutoffs.

*Geometry correlation lengths.* A key requirement is that the geometry should act as a regulator rather than a critical field. We therefore measure two complementary correlators: (i) a displacement correlator based on  $u(n) = x(n) - an$ , with the configurationwise mean subtracted to remove the translation zero mode, and (ii) the connected volume–volume correlator  $C_V(r)$  defined in §5.2, binned by graph distance. Both decay rapidly and are consistent with short–range geometry fluctuations, cf. Fig 3g–3h.

In plots we show  $|C_V(r)|$  on a log scale and extract an effective decay length  $\ell_{\text{geom}}$  from an exponential fit over short to intermediate  $r$ . Across the volumes tested, the fitted decay length stays  $O(1)$  in lattice units with no systematic growth in  $L$  (e.g.  $\ell_{\text{geom}} \approx 1.34, 0.99, 0.54, 0.92$  for  $L = 16, 24, 32, 48$  at  $\mu^2 \simeq -1.40$ ). This provides direct numerical support for (SR) in this two–dimensional test.

## 5.4 Thermalisation and stability

Figures 4a and 4b show time-series diagnostics for representative baseline and dynamical runs. After the thermalisation window the actions and low moments fluctuate around stationary means with no visible long-term drift. Figure 4a records the evolution of the minimum cell area and the maximum aspect ratio over the lattice; both remain stable throughout the production window, with no signs of slow drift or metastability, indicating that the geometry explores the admissible region rather than getting trapped near a boundary.

## 5.5 Rotational artefacts: short and intermediate scales

*Angle-binned gradients.* On the fixed square lattice  $H(\theta)$  exhibits a clear fourfold pattern, while on the dynamical ensemble the modulation is strongly reduced (Fig. 4e). Table 2 summarises this via  $A_{\text{rms}}$  and  $A_4$ . Quantitatively,  $A_{\text{rms}}$  drops from 0.42 to 0.12 (a factor  $\approx 3.5$ ), while  $A_4$  drops from 0.17 to 0.08 (a factor  $\approx 2.2$ ), indicating substantial suppression of the dominant fourfold harmonic in this short-distance diagnostic.

Regulator	$A_{\text{rms}}$	$A_4$
Baseline	0.4221(1)	0.1729(1)
Dynamical	0.1207(3)	0.0787(2)

Table 2: Anisotropy measures from the angle-binned gradient observable ( $\mu^2 = -1.34$ ,  $L = 48$ ).

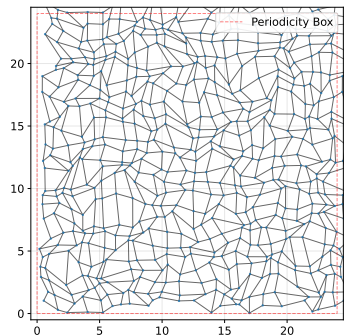
*Directional two-point functions.* As a longer-distance probe we compare axis-like and diagonal-like two-point functions. The difference  $\Delta G(r) = G_{\text{diag}}(r) - G_{\text{axis}}(r)$  is a compact diagnostic of residual directional splitting. Figure 4c shows that the baseline regulator exhibits a modest but systematic non-zero signal at short to intermediate distances, whereas in the dynamical ensemble  $\Delta G(r)$  is consistent with zero over the range where  $G(r)$  is still clearly above the noise floor.

For completeness we also show the underlying correlators  $G_{\text{axis}}(r)$  and  $G_{\text{diag}}(r)$  in Fig. 4d; the difference plot above contains the main rotational-symmetry information in a more sensitive form.

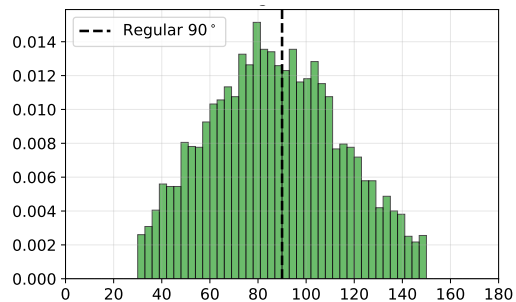
## 5.6 Universality and critical scaling

Finally, we check that coupling the scalar theory to the DLR geometry does not change its long-distance universality class. We simulate  $L \in \{16, 24, 32, 48\}$  and scan the bare mass parameter  $\mu^2$  at fixed quartic coupling (here  $\lambda = 1$ ) using the protocol of Section 5.1. Figure 4f shows the Binder cumulant and  $\xi/L$  as functions of  $\mu^2$  for the dynamical ensemble. Both observables exhibit a common crossing region near  $\mu_c^2 \simeq -1.40$ , as expected for a second-order transition. The Binder value at the crossing is consistent with the 2D Ising universality class; since the baseline square-lattice  $\phi^4$  theory is known to lie in the same class, this supports the conclusion that the coupled geometry does not modify the long-distance universality in this two-dimensional test.

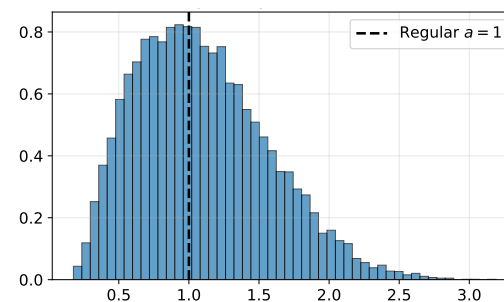
We estimate integrated autocorrelation times for  $M^2$  and observe the expected critical slowing down with  $L$ ; at  $\mu^2 \approx -1.40$  we find  $\tau_{M^2} \approx (1.4, 4.0, 5.2, 8.5) \times 10^2$  sweeps for  $L = 16, 24, 32, 48$ . Accordingly, error bars are obtained with blocking/binning using block sizes  $\gg \tau_{M^2}$  and by averaging over multiple independent seeds. As a basic check on the geometry sector, we also monitored autocorrelations of simple global geometry summaries (e.g.  $\sum_n A(n)$  and  $\sum_n S_x(n)$ ) and found no anomalously slow mode in the runs shown.



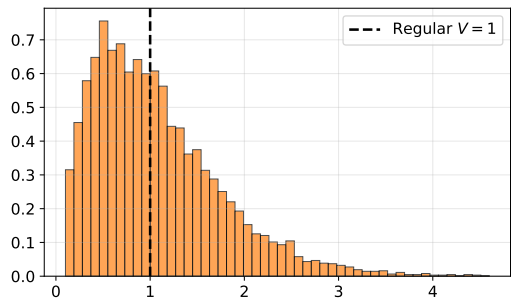
(a) Typical embedded mesh.



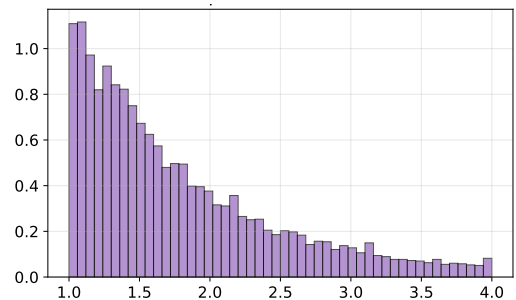
(b) Corner angle distribution.



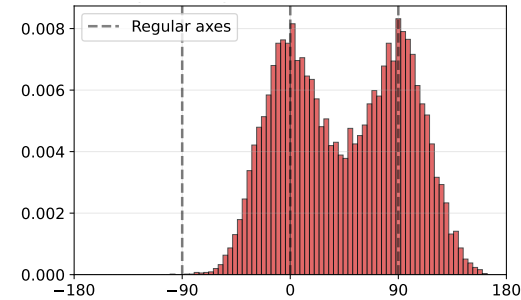
(c) Edge-length distribution.



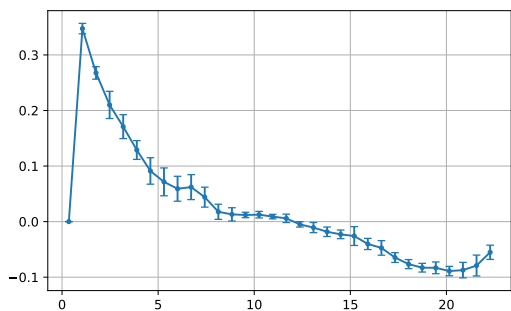
(d) Cell-area distribution.



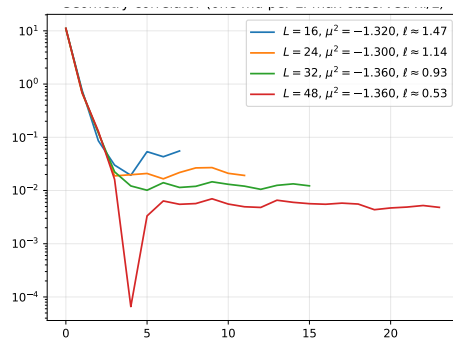
(e) Aspect-ratio distribution.



(f) Edge orientations.

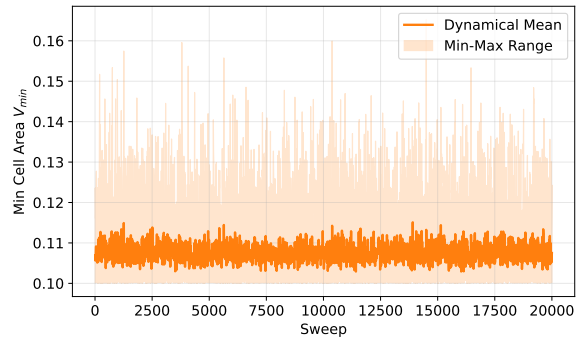


(g) Displacement correlator.

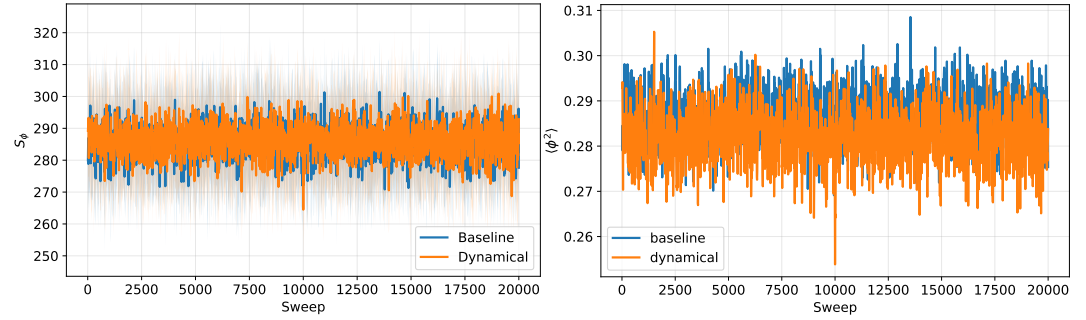


(h) Volume correlator.

Figure 3: Geometry diagnostics for the dynamical ensemble (all panels at identical scale).



(a) Geometry stability: min area / max aspect.



(b) Time series: actions and scalar moments.

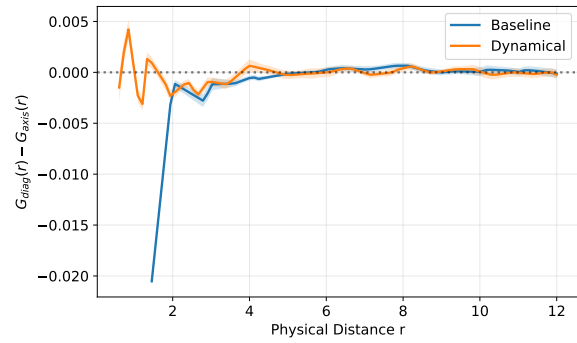
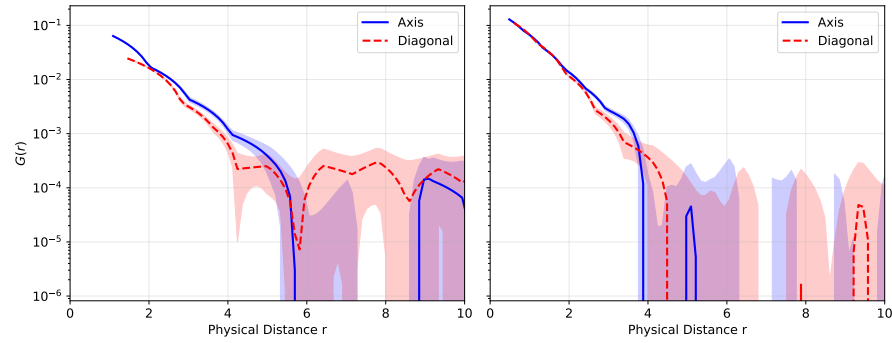
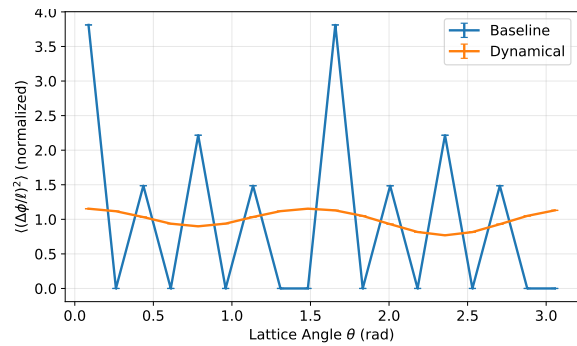
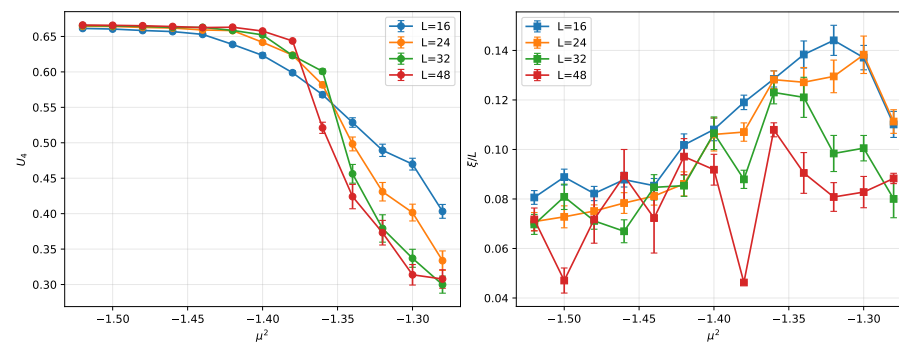
(c) Directional splitting  $\Delta G(r)$ .(d) Directional correlators  $G_{\text{axis}}, G_{\text{diag}}$ .(e) Angle-binned gradient profile  $H(\theta)$ .(f) Universality checks:  $U_4$  and  $\xi/L$ .

Figure 4: Matter, rotational-symmetry, and stability diagnostics comparing baseline and dynamical ensembles.

## 6 Conclusions and outlook

In this paper we established that the dynamical–lattice regulator (DLR) provides a local, gauge-invariant cutoff that is exactly  $SE(d)$ –covariant at finite lattice spacing, and admits Osterwalder–Schrader reflection positivity (hence a standard transfer-matrix reconstruction) for a broad class of coupled geometry–field actions. Assuming the short-range geometry hypothesis (SR), integrating out  $x$  at fixed  $a$  yields a local Symanzik effective action in which geometry fluctuations generate only  $SO(d)$ –invariant irrelevant operators (and finite renormalisations), a mechanism checked explicitly at one loop in scalar  $\phi^4$ . Our  $d = 2$  Monte Carlo tests provide proof-of-concept evidence for stable short-range geometry near matter criticality, reduced rotational artefacts at finite cutoff, and matching critical scaling with the baseline theory.

From the lattice–QCD viewpoint, DLR may be regarded as an *annealed geometric averaging in coordinate space* that preserves the transfer–matrix/reflection–positivity framework, complementary to field–space smoothing techniques (smearing, gradient flow) that improve operators/observables but do not on their own define a new reflection–positive cutoff. Structurally, DLR also occupies a conservative middle ground between rigid hypercubic regulators and fluctuating–topology approaches such as random lattices and dynamical triangulations: the abstract connectivity is fixed (so reflection positivity and standard lattice algorithms remain accessible), while the embedding fluctuates with a local action *inside* the same path integral as the gauge and matter fields.

### 6.1 Future directions

There are several natural directions in which the present work can be extended.

- *Systematic numerical studies.* The exploratory scalar simulations in Section 5 should be developed into a systematic study of rotational symmetry restoration, autocorrelations and finite–size effects, and extended to gauge theories in  $d = 3, 4$ . In the gauge sector this should include standard benchmarks such as plaquette distributions, gradient–flow scales, the static quark potential and string tension (including the Lüscher term), as well as diagnostics of topological objects and topological–charge autocorrelations (topology freezing) and their sensitivity to grid artefacts. A quantitative comparison of anisotropy diagnostics and scaling violations between static and dynamical meshes would clarify the practical gains of the regulator.
- *Geometry phase structure in 4d and the short–range hypothesis.* The viability of DLR as a regulator hinges on an operating window in which the geometry sector remains short-range (SR) after fixing the global  $SE(d)$  zero modes: connectivity is fixed and nondegenerate, yet local orientations remain disordered. While the  $d = 2$  scalar experiments provide evidence consistent with such a regime even for a minimal geometry action, in  $4d$  this is not guaranteed: competing entropic regimes (e.g. crystallisation/orientational ordering or, at the opposite extreme, crumpling–type instabilities familiar from random geometry models) may appear unless suitable stiffness terms and admissibility thresholds are chosen. A priority for  $4d$  applications is therefore to map the geometry phase diagram as a function of these parameters, using geometry correlators and autocorrelation times as diagnostics.
- *Fermions and chiral symmetry.* In this first work we have not addressed the question of fermion doubling in detail. Since the dynamical mesh restores exact  $SE(d)$  symmetry but

does not change the local Dirac operator on the abstract lattice, one expects the usual no-go theorems to continue to apply. Nonetheless, it would be worthwhile to investigate systematically how standard fermion formulations (Wilson, staggered, overlap) behave in the presence of a fluctuating geometry, and to quantify whether averaging over the mesh reduces rotational artefacts such as taste splitting in staggered fermions, effectively isotropising the doubler spectrum even if their number is preserved.

- *Quenched geometry and “quantum adaptivity”.* Besides the annealed formulation studied here, it would be interesting to consider a *quenched* variant in which the abstract hypercubic connectivity is fixed and the embedding  $x(n) = an + \eta(n)$  is sampled independently from an  $SE(d)$ -invariant short-range law, after which gauge and matter fields are simulated conditionally on  $x$  and observables are averaged over the geometry ensemble. This quenched perspective removes geometric backreaction and may therefore be more amenable to analytic control. Conversely, in the annealed theory the fields can bias the geometry measure; it is an interesting possibility that this backreaction acts as a kind of *quantum adaptivity*, with the auxiliary embedding degrees of freedom tending to adjust locally in response to field configurations, potentially reducing certain cutoff artefacts.
- *Hamiltonian formulation.* An important direction is to develop a Kogut–Susskind–type Hamiltonian version of DLR. Given Osterwalder–Schrader reflection positivity and the transfer matrix interpretation of the Euclidean theory, one expects a canonical description in which geometry variables appear as additional degrees of freedom on time slices and modify the electric and magnetic terms only via local geometry-dependent couplings.
- *Other topologies and simplicial variants.* While we have focused on a hypercubic abstract lattice for constructive and algorithmic reasons, a simplicial version of DLR would be natural and would connect more directly to Regge calculus. One could also consider other topologies (e.g. manifolds with boundaries, or nontrivial spatial topology) as long as a suitable notion of admissible embeddings and OS reflection exists.
- *Coupling to dynamical gravity.* Finally, one may contemplate turning the auxiliary geometry sector into a genuine gravitational degree of freedom by adding a Regge-type curvature term to  $S_x[x]$  and allowing the geometry to fluctuate on large scales. This would blur the distinction between “regulator geometry” and “physical geometry”, and might provide a technically conservative route towards combining lattice gauge theory with discrete approaches to quantum gravity. Such questions are, however, well beyond the scope of the present paper.

We view the present work as a starting point, and we invite further numerical and analytical tests of DLR, in particular in  $d = 4$  where establishing (SR) and benchmarking rotational artefacts against standard improvement and flow-based techniques are decisive.

## Acknowledgements

This work was supported by NSERC Discovery Grants Program.

## References

- [1] K. G. Wilson, “Confinement of quarks,” *Phys. Rev. D* **10** (1974), 2445–2459.

- [2] J. B. Kogut, “An introduction to lattice gauge theory and spin systems,” *Rev. Mod. Phys.* **51** (1979), 659–713.
- [3] H. J. Rothe, *Lattice Gauge Theories: An Introduction*, 4th ed., World Scientific, Singapore, 2012.
- [4] N. H. Christ, R. Friedberg, and T. D. Lee, “Random lattice field theory: General formulation,” *Nucl. Phys. B* **202** (1982), 89–125.
- [5] N. H. Christ, R. Friedberg, and T. D. Lee, “Weights of links and plaquettes in a random lattice,” *Nucl. Phys. B* **210** (1982), 337–346.
- [6] P. Colangelo and E. Scrimieri, “Gauge theories on a pseudorandom lattice,” *Phys. Rev. D* **35** (1987), 3193.
- [7] P. Colangelo, L. Cosmai, and E. Scrimieri, “Computer simulation of gauge theories on a lattice with improved rotational symmetry,” *Comput. Phys. Commun.* **54** (1989), 235–237.
- [8] T. Regge, “General relativity without coordinates,” *Nuovo Cimento* **19** (1961), 558–571.
- [9] H. W. Hamber, “Quantum gravity on the lattice,” *Gen. Relativ. Gravit.* **41** (2009), 817–876.
- [10] J. Ambjørn, B. Durhuus, and T. Jonsson, *Quantum Geometry: A Statistical Field Theory Approach*, Cambridge University Press, Cambridge, 1997.
- [11] J. Ambjørn, J. Jurkiewicz, and R. Loll, “Dynamically triangulating Lorentzian quantum gravity,” *Nucl. Phys. B* **610** (2001), 347–382.
- [12] M. Albanese *et al.* (APE Collaboration), “Glueball masses and string tension in lattice QCD,” *Phys. Lett. B* **192** (1987), 163–169.
- [13] C. Morningstar and M. Peardon, “Analytic smearing of SU(3) link variables in lattice QCD,” *Phys. Rev. D* **69** (2004), 054501.
- [14] A. Hasenfratz and F. Knechtli, “Flavor symmetry and the static potential with hypercubic blocking,” *Phys. Rev. D* **64** (2001), 034504.
- [15] M. Lüscher, “Properties and uses of the Wilson flow in lattice QCD,” *JHEP* **08** (2010), 071.
- [16] K. Symanzik, “Continuum limit and improved action in lattice theories: (I). Principles and  $\phi^4$  theory,” *Nucl. Phys. B* **226** (1983), 187–204.
- [17] K. Symanzik, “Continuum limit and improved action in lattice theories: (II).  $O(N)$  nonlinear sigma model in perturbation theory,” *Nucl. Phys. B* **226** (1983), 205–227.
- [18] C. J. Budd, W. Huang, and R. D. Russell, “Adaptivity with moving grids,” *Acta Numer.* **18** (2009), 111–241.
- [19] W. Huang and R. D. Russell, *Adaptive Moving Mesh Methods*, Applied Mathematical Sciences Vol. 174, Springer, New York, 2011.
- [20] K. Osterwalder and R. Schrader, “Axioms for Euclidean Green’s functions,” *Commun. Math. Phys.* **31** (1973), 83–112.



- [21] K. Osterwalder and R. Schrader, “Axioms for Euclidean Green’s functions II,” *Commun. Math. Phys.* **42** (1975), 281–305.
- [22] M. Lüscher, “Construction of a selfadjoint, strictly positive transfer matrix for Euclidean lattice gauge theories,” *Commun. Math. Phys.* **54** (1977), 283–292.
- [23] K. Osterwalder and E. Seiler, “Gauge field theories on the lattice,” *Ann. Phys.* **110** (1978), 440–471.
- [24] H. B. Nielsen and M. Ninomiya, “No-go theorem for regularizing chiral fermions,” *Phys. Lett. B* **105** (1981), 219–223.
- [25] K. G. Wilson, “Quarks and strings on a lattice,” in *New Phenomena in Subnuclear Physics*, ed. A. Zichichi, Plenum, New York, 1977, pp. 69–142.